



## King's Research Portal

DOI:  
[10.3791/64063](https://doi.org/10.3791/64063)

*Document Version*  
Peer reviewed version

[Link to publication record in King's Research Portal](#)

*Citation for published version (APA):*

Attwaters, M., Kelu, J. J., Pipalia, T., & Hughes, S. M. (2022). Real Time and Repeated Measurement of Skeletal Muscle Growth in Individual Live Zebrafish Subjected to Altered Electrical Activity. *Journal of visualized experiments : JoVE*, 2022(184), 1-23. Article e64063. <https://doi.org/10.3791/64063>

### **Citing this paper**

Please note that where the full-text provided on King's Research Portal is the Author Accepted Manuscript or Post-Print version this may differ from the final Published version. If citing, it is advised that you check and use the publisher's definitive version for pagination, volume/issue, and date of publication details. And where the final published version is provided on the Research Portal, if citing you are again advised to check the publisher's website for any subsequent corrections.

### **General rights**

Copyright and moral rights for the publications made accessible in the Research Portal are retained by the authors and/or other copyright owners and it is a condition of accessing publications that users recognize and abide by the legal requirements associated with these rights.

- Users may download and print one copy of any publication from the Research Portal for the purpose of private study or research.
- You may not further distribute the material or use it for any profit-making activity or commercial gain
- You may freely distribute the URL identifying the publication in the Research Portal

### **Take down policy**

If you believe that this document breaches copyright please contact [librarypure@kcl.ac.uk](mailto:librarypure@kcl.ac.uk) providing details, and we will remove access to the work immediately and investigate your claim.

# Journal of Visualized Experiments

## Real time and repeated measurement of skeletal muscle growth in individual live zebrafish subjected to altered electrical activity

--Manuscript Draft--

<b>Article Type:</b>	Invited Methods Article - JoVE Produced Video
<b>Manuscript Number:</b>	JoVE64063R1
<b>Full Title:</b>	Real time and repeated measurement of skeletal muscle growth in individual live zebrafish subjected to altered electrical activity
<b>Corresponding Author:</b>	Simon M. Hughes King's College London London, UNITED KINGDOM
<b>Corresponding Author's Institution:</b>	King's College London
<b>Corresponding Author E-Mail:</b>	s.hughes@kcl.ac.uk;simon.hughes@kcl.ac.uk
<b>Order of Authors:</b>	Michael Attwaters Jeffrey J. Kelu Tapan G. Pipalia Simon M. Hughes
<b>Additional Information:</b>	
<b>Question</b>	<b>Response</b>
Please specify the section of the submitted manuscript.	Developmental Biology
Please indicate whether this article will be Standard Access or Open Access.	Open Access (\$3900)
Please indicate the <b>city, state/province, and country</b> where this article will be <b>filmed</b> . Please do not use abbreviations.	London UK
Please confirm that you have read and agree to the terms and conditions of the author license agreement that applies below:	I agree to the <a href="#">UK Author License Agreement</a> (for UK authors only)
Please confirm that you have read and agree to the terms and conditions of the video release that applies below:	I agree to the <a href="#">Video Release</a>
Please provide any comments to the journal here.	As discussed with Benjamin Werth, this article is using the publication grant from the Methods Collection of Julien Bergeron

1

2 **TITLE:**

3 Real time and repeated measurement of skeletal muscle growth in individual live zebrafish  
4 subjected to altered electrical activity

5

6

7 **AUTHORS AND AFFILIATIONS:**

8 Michael Attwaters<sup>1</sup>, Jeffrey J. Kelu<sup>1</sup>, Tapan G. Pipalia and Simon M. Hughes\*

9 Randall Centre for Cell and Molecular Biophysics, School of Basic and Medical Biosciences, King's  
10 College London SE1 1UL, UK.

11 <sup>1</sup> These authors contributed equally

12 \*Correspondence to: [s.hughes@kcl.ac.uk](mailto:s.hughes@kcl.ac.uk)

13

14 **SUMMARY:**

15

16 Optical clarity is a major advantage for cell biological and physiological work in zebrafish. Robust  
17 methods for measurement of cell growth in individual animals are described that permit novel  
18 insights into how growth of skeletal muscle and neighbouring tissues are integrated with whole  
19 body growth.

20

21

22 **ABSTRACT:**

23

24 A number of methods can be used to visualize individual cells throughout the body of live  
25 embryonic, larval or juvenile zebrafish. We show that live fish with fluorescently-marked plasma  
26 membranes can be scanned in a confocal laser scanning microscope in order to determine the  
27 volume of muscle tissue and the number of muscle fibres present. Efficient approaches for the  
28 measurement of cell number and size in live animals over time are described and validated  
29 against more arduous segmentation methods. Methods are described that permit the control of  
30 muscle electrical, and thus contractile, activity. Loss of skeletal muscle contractile activity greatly  
31 reduced muscle growth. In larvae, a protocol is described that allows reintroduction of patterned  
32 electrical-evoked contractile activity. The described methods minimize the effect of inter-  
33 individual variability and will permit analysis of the effect of electrical, genetic, drug, or  
34 environmental stimuli on a variety of cellular and physiological growth parameters in the context  
35 of the living organism. Long-term follow-up of the measured effects of a defined early-life  
36 intervention on individuals can subsequently be performed.

37

38

39

40

41

42

43

44

45 **INTRODUCTION:**

46

47 Regulated tissue growth, comprising increase in cell number (hyperplasia) and/or cell size  
48 (hypertrophy), is a crucial factor in development, regeneration and ecological and evolutionary  
49 adaptation. Despite huge advances in molecular genetic understanding of both cell and  
50 developmental biology over recent decades, mechanistic understanding of the regulation of tissue  
51 and organ size is still in its infancy. One reason for this lacuna in knowledge is the difficulty of  
52 quantifying tissue growth in living organisms with the necessary spatial and temporal accuracy.

53

54 Various aspects of growth of whole organisms can be measured repeatedly over time, revealing  
55 growth curves for each individual <sup>1-5</sup>. Increasingly sophisticated scanning methods, such as dual  
56 X-ray absorptiometry (DXA), computerized tomography (CT) and magnetic resonance imaging  
57 (MRI), permit the tracking of growth of whole organs and other body regions (for example,  
58 individual identified skeletal muscles) in single individuals, both human and in model organisms  
59 <sup>6-10</sup>. However, these methods do not yet have the resolution to reveal individual cells and thus the  
60 links between cellular behaviours and tissue level growth have been hard to discern. To make  
61 such links, traditional studies have often relied upon cohorts of similar individual animals, a few  
62 of which are sacrificed at successive timepoints and then analysed in cytological detail. Such  
63 approaches require averaging the observed changes across groups of (preferably similar, but  
64 nevertheless variable) individuals and thus suffer from a lack of temporal and spatial resolution,  
65 making it hard to find correlated events at the cellular level suggestive of cause and effect.

66

67 Studies on invertebrate model organisms, initially in *C. elegans* and *D. melanogaster*, have  
68 circumvented these problems by developing optical microscopy to achieve cellular resolution and  
69 accurately measure growth over time in single individuals. Such studies have revealed strikingly  
70 invariant cell lineage behaviours in the growth of these small model organisms <sup>11-17</sup>. However,  
71 many animals, including all vertebrates, have indeterminate cell lineages, and control tissue  
72 growth by mysterious feedback processes that serve to turn the genetically-encoded growth  
73 program into a functional three dimensional organism with all its constituent tissues and organs  
74 suitably matched in size. To understand these complex growth processes, it is desirable to image  
75 whole tissues or organs over time in single individuals that can be experimentally manipulated by  
76 genetic, pharmacological or other interventions at a time of choice and the effect subsequently  
77 analysed.

78

79 Each vertebrate skeletal muscle has a defined size, shape and function and well-characterised  
80 interactions with adjacent tissues, such as bone, tendon and nerves. Some muscles are small, lie  
81 just under the skin and are therefore good candidates for high-resolution imaging studies. Like  
82 most organs, each muscle grows throughout embryonic, postnatal and juvenile life, before  
83 reaching a stable adult size. Muscle, however, also has a unique ability to change size during  
84 adult life, dependent upon use and nutrition <sup>18</sup>, and this property has a major impact on organismal  
85 fitness, sporting performance and independent living. Loss of muscle mass and function in old  
86 age, sarcopenia, is an issue of increasing concern for societies faced with an ageing population  
87 <sup>19-21</sup>.

88

89 We and others have focused on the growth of defined blocks of skeletal muscle tissue in the  
90 segmentally-repeating body of zebrafish larvae, as an apparently closed system containing  
91 several hundred cells in which tissue growth, maintenance and repair can be observed and  
92 manipulated <sup>22-26</sup>. While some quantitative work has previously been reported <sup>25-35</sup>, no detailed  
93 and validated method of measuring muscle growth in cellular detail in individual vertebrate  
94 organisms over time is available. Here an efficient protocol for how to perform such repeated

95 measurements is described, along with validation, and an example of its use to analyse changes  
96 in both hypertrophic and hyperplastic growth in response to altered electrical activity is provided.

## 99 **PROTOCOL:**

100  
101 All research described was performed in compliance with institutional guidelines and under  
102 suitable licences from UK Home Office in accordance with the Animal (Scientific Procedures) Act  
103 1986 and subsequent modifications. Embryos/larvae should be reared at 28.5°C until completion  
104 of gastrulation, but may then be kept at 22-31°C to control the rate of development. Fish may be  
105 scanned or stimulated at room temperature.

### 108 **1. Anaesthetise zebrafish larvae**

- 110 1.1. Cross suitable fluorescent reporter adult fish such as *Tg(Ola.Actb:Hsa.HRAS-*  
111 *EGFP)<sup>vu119Tg</sup>* ref.<sup>36</sup> or *Tg( $\alpha$ -actin:mCherry-CAAX)<sup>pc22Tg</sup>* ref.<sup>37</sup> and collect embryos as  
112 described<sup>38</sup>.
- 113 1.2. At time of choice, such as 2 days post-fertilization (dpf), anaesthetise embryos briefly  
114 using Tricaine-containing fish medium (either fish water or E3 medium), and screen for  
115 EGFP or mCherry under a fluorescence microscope, such as a Leica MZ16F. If one has  
116 many embryos, select those with the brightest signal. Return embryos to normal fish  
117 medium immediately after screening.

### 118 **2. Mounting fish for confocal scanning**

- 121 2.1. Turn on the confocal laser scanning system and lasers, to let system stabilize for 30-60  
122 min. A Zeiss LSM 5 Exciter microscope with an upright Materials stand (which enhances  
123 working distance) equipped with 20x/1.0W water-immersion objective may be used.
- 124 2.2. Freshly prepare 1% low melting agarose (LMA) and keep in a 37°C heat block for  
125 repeated use in a 1.5 mL 'Eppendorf' tube. To avoid heat-shock, it is best to let the LMA  
126 aliquot cool to just above setting before applying to the larva. Remove the tube containing  
127 the LMA from the heat block and allow it to cool, testing against one's skin to judge the  
128 appropriate temperature, as when assessing the temperature of baby formula milk.
- 129 2.3. Select fish to be mounted and transiently anaesthetise each fish in turn with Tricaine  
130 (0.6 mM in fish medium).
- 131 2.4. Take a 60 mm diameter Petri dish that has been coated with a layer of 1% agarose and  
132 place on stage of a dissecting microscope.
- 133 2.5. Transfer the larva with a 1 mL plastic Pasteur pipette onto the 60 mm coated Petri dish  
134 and remove as much transferred medium as possible. Then, still using the Pasteur  
135 pipette, place 5 to 10 drops of LMA onto the fish and rapidly position horizontally in lateral  
136 view with forceps (or a fire-polished fine glass needle) before the LMA sets.
- 137 2.6. Alternatively, using a 1 mL plastic Pasteur pipette, collect the larva with as little fish  
138 medium as possible, and transfer the larva into the aliquot of barely-liquid LMA. Allow  
139 the larva to sink for 5 s to become fully surrounded by LMA, then retrieve the larva and  
140 transfer it in a drop of LMA onto the agarose-coated Petri dish. Quickly orientate and  
141 position the larva as described above.
- 142 2.7. It is highly desirable to orient the larva with both its anteroposterior and dorsoventral axes  
143 within 10° of horizontal (see Note: On error and its correction at point 4.5 below). If larva  
144 is not correctly mounted horizontally near the surface of the agarose drop, it is better to

145 remove and re-embed. Larvae can be easily retrieved by gentle suction using a microfine  
146 1 mL plastic Pasteur pipette, and LMA can be gently removed using Kimwipes. Practice  
147 really does make perfect in the mounting procedure; spend an afternoon embedding  
148 some unimportant larvae before trying this on a real experiment.

149 **NOTE:** On microscope design. Many labs use inverted confocal microscopes for imaging  
150 through a coverslip. We have found that the repeated embedded and removal of fish held in  
151 agarose under a coverslip for observation in an inverted microscope leads to greater loss of  
152 samples during repeated scanning than in the described procedure with an upright  
153 microscope. For this reason, the use of an upright system is recommended, if available.  
154 Nevertheless, a key to high quality data is the proper selection and use of objective and scan  
155 parameters, a subject too large for discussion here.

156

### 157 3. Confocal scanning

158

159 3.1. When LMA has set, flood the dish with around 10 mL of Tricaine-containing fish medium.  
160 If planning to capture confocal stacks, let the mounted fish rest for at least 10 min before  
161 proceeding to scanning, as some agarose swelling occurs.

162 3.2. Load sample dish to the stage of the confocal system, locate larva and focus on desired  
163 somite. Somite 17 may be chosen because of its ease of localization near the anal vent  
164 and ease of imaging. Check by counting somites from anterior. **NOTE:** the first somite  
165 is fused behind the ear and has no anterior border, but can be readily observed to have  
166 striated muscle fibres.

167 3.3. Set up as if to capture a Z-stack by defining top (i.e. just above the skin) and bottom (i.e.  
168 just below the notochord, so as to include the entire somite, even if the fish is mounted  
169 slightly skewed). Both left and right sides can be captured as desired. This will ensure  
170 that all the rapid YZ scans capture the desired region(s).

171 3.4. Capture an XY image. Orient the scan area with respect to the fish, as the confocal  
172 software permits. The fish is positioned with the anteroposterior axis parallel to the  
173 imaged X axis and dorsoventral axis parallel to the Y axis with somite 17 in the centre of  
174 the field as shown in **Supplementary File 1**. Focus on a mid-level plane in the uppermost  
175 myotome in which the whole epaxial and hypaxial somite halves together with the vertical  
176 and horizontal myosepta are visible and capture a high resolution XY image. Remember  
177 to name and save the image.

178 3.5. Capture one or more YZ images as follows. In the Representative Results (below) the  
179 accuracy of '2-slice' and '4-slice' methods is compared. In the 2-slice approach, single  
180 XY and YZ scans are employed. In the 4-slice approach, three YZ scans are averaged  
181 to give a more accurate estimate of myotome volume. If required by the confocal  
182 software, re-orient the scan field. Draw a precisely dorsal to ventral line across the  
183 chosen somite perpendicular to the fish anteroposterior axis at a selected anteroposterior  
184 position. Perform a Z-stack line scan. Repeat the YZ line scan three times at defined  
185 anteroposterior positions along the selected myotome to capture *YZ<sub>a</sub>*, *YZ<sub>m</sub>* and *YZ<sub>p</sub>*.  
186 Representative results are shown in Figure 2A. Name and save these images together  
187 with the related XY image.

188 **Note:** On selection of YZ planes. The myotome is V-shaped and its form changes during  
189 growth. To obtain the most accurate assessment of myotome 17 volume with the 4-slice  
190 method, position *YZ<sub>a</sub>* on the anterior tip of the myotome, *YX<sub>p</sub>* on the posterior tips of the  
191 myotome at dorsal and ventral extremes and *YX<sub>m</sub>* halfway between *YZ<sub>a</sub>* and *YZ<sub>p</sub>*. Assuming  
192 the somite tapers uniformly, the mean of measurements from each YZ section will represent  
193 the myotome as a whole. For the 2-slice method, the single YZ scan should be positioned at  
194 the posterior end of the horizontal myoseptum, which roughly corresponds to the  
195 anteroposterior centre of the myotome of interest (like *YZ<sub>m</sub>*). Alternatively, a set of three YZ

sections may be taken at anterior, middle and posterior of horizontal myoseptum but, as shown below, such measurement will slightly over- or under-estimate myotome volume (for rostral and caudal somites, respectively, due to myotome tapering). Fundamentally, consistency in positioning of YZ slice plane(s) between fish and experiments is key to reproducibility.

#### 4. Analysis

4.1. As the myotome changes size along the fish in a graded manner, it is essential to always work with the same somite in comparative studies.

4.2. To measure and calculate the myotome volume, use the confocal software (such as the '.ism' files created using Zeiss ZEN microscope software) or open-source universal image analysis software, such as Fiji/ImageJ (National Institutes of Health, NIH). *NOTE:* if changing file formats, make sure the Z-step size is correctly transferred, as not all software can read proprietary confocal file formats correctly. For example, to import a ZEN line scan image into Fiji, first use the File/Export command to export as '.tif' in the 'Full resolution image window – single plane' format, then import into Fiji. Although 'YZ scan.ism' can be opened directly in Fiji, the resulting YZ images are generally compressed in the 'Z' dimension due to incorrect evaluation of the Z step size.

##### 4.3. Analysis using ZEN.

4.3.1. First, open the 'XY scan.ism' files in ZEN. Go to the 'Graphics' tab and select the 'Line' tool. Draw a line between the two vertical myosepta of somite 17 spanning the entire the myotome length (parallel to the anteroposterior axis of the fish). Check the 'M' box to reveal the values of the measurement (Length = 89.71  $\mu\text{m}$ , see **Supplemental File 2**).

4.3.2. Open the 'YZ scan.ism' files. Under the 'Graphics' tab, select the 'Closed bezier' tool. Draw around the perimeter of the myotome. Once completed, check the 'M' box, this would reveal the value of the measurement (Area = 11980.01  $\mu\text{m}^2$ , see **Supplemental File 3**).

4.3.3. Record the values of each measurement manually in a Microsoft Excel spreadsheet or similar. Average the CSA measurements as required. Volume of the myotome can be calculated as Volume = Myotome length  $\times$  CSA. i.e.  $89.71 \mu\text{m} \times 11980.01 \mu\text{m}^2 = 1.075 \times 10^6 \mu\text{m}^3$ .

##### 4.4. Analysis using Fiji/ImageJ.

4.4.1. Open the 'XY scan.ism' files in Fiji/ImageJ. Check that XY images directly opened in Fiji are correctly calibrated in scale, as they should be.

4.4.2. Select the 'Straight Line' tool from the icons. Draw a line along the length of somite 17 as described in 4.3.1. Set measurement parameters by going to 'Analyze', then select 'Set Measurements...', and check the following boxes 'Area' and 'Display label'. To measure, simply press the hot key 'M', or go to 'Analyze' menu and select 'Measure'. A resulting pop-up window lists all measurement values (i.e. Length = 90.023  $\mu\text{m}$ ; see **Supplemental File 4**). The results can be saved in form of '.csv' and opened in Microsoft Excel or similar for subsequent analysis.

4.4.3. To measure CSA on the YZ images, open YZ images in '.tif' format as described in 4.2.

4.4.4. Calibrate the YZ '.tif' images as they are uncalibrated when exported. Parameters for the calibration can be obtained in ZEN by going to the 'Info' of the selected images: record the 'Scaling X' (0.489  $\mu\text{m}$ ) and 'Scaling Z' values (0.890  $\mu\text{m}$ ; see **Supplemental File 5**). Next, while the images are open in Fiji, go to 'Image' and select 'Properties...'. Input '0.489  $\mu\text{m}$ ' for the 'Pixel width' and 'Pixel height' and '0.890  $\mu\text{m}$ ' for the 'Voxel depth'. Check the 'Global' box to apply the calibration

247 universally if repeated measurement of YZ images is anticipated (see **Supplemental**  
248 **File 6**). *NOTE:* Make sure all YZ images are captured using the same scanning  
249 parameters; restart Fiji/ImageJ or modify the calibration values if a new set of  
250 calibration is required.

251 4.4.5. To measure the CSA of the calibrated YZ images, select the 'Polygon selections'  
252 tool from the icons. Draw around the perimeter of the somite, and press 'M' to reveal  
253 the values of the measurement (Area = 11980.395  $\mu\text{m}^2$ ; see **Supplemental File 7**).  
254 Volume of the myotome can be calculated as Volume = Myotome length  $\times$  CSA. i.e.  
255  $90.023 \mu\text{m} \times 11980.395 \mu\text{m}^2 = 1.079 \times 10^6 \mu\text{m}^3$ .

256 4.5 Repeat the measurements on the other XY and YZ images. It is recommended to use  
257 the same software for all measurements within an experimental series for consistency.  
258 The volume estimate from each software is similar but not identical due to the distinct  
259 drawing tools i.e. ZEN =  $1.074 \times 10^6 \mu\text{m}^3$  and Fiji/ImageJ =  $1.079 \times 10^6 \mu\text{m}^3$ . Growth of  
260 the myotome between two time points (i.e. 3 to 4 dpf) can be calculated as: (Volume<sub>4 dpf</sub> -  
261 Volume<sub>3 dpf</sub>) / Volume<sub>3 dpf</sub>  $\times$  100%.

262 *NOTE:* On error and its correction. During mounting, the fish should be orientated with its  
263 sagittal plane (i.e. the anteroposterior and dorsoventral axes) as close as possible to  
264 horizontal, to avoid yaw and roll, respectively. This is because both the myotome length  
265 L measured from the XY scan and the CSA measured from a YZ scan will be over-  
266 estimated if the fish shows yaw (rotation around the dorsoventral axis) due to oblique  
267 anteroposterior mounting. Neither pitch nor roll during mounting should affect  
268 measurements after scanning as described in section 3. Nevertheless, dorsoventral  
269 rotation (roll) degrades image quality. Simple trigonometry shows that up to  $10^\circ$  of yaw will  
270 give 3% error in volume measurement, as measured L and CSA each increase in  
271 proportion to  $(\cos\theta)^{-1}$ , where  $\theta$  is the angle away from anteroposterior horizontal (yaw).  
272  $15^\circ$  and  $20^\circ$  off will give 7% and 13% over-estimates of volume, respectively.

273 As the notochord is cylindrical, inclusion of the whole notochord in the YZ scan can be  
274 used to calculate the angle and extent of obliquity from the orientation and magnitude of  
275 the major and minor axes and thereby correct the measured L and CSA to maximize  
276 accuracy. Corrected CSA = Measured CSA  $\times$  Notochord minor axis / Notochord major axis.  
277 Corrected L = Measured L  $\times$  Notochord minor axis / Notochord axis in microscope Z  
278 direction.

279 A further consideration permits additional correction of L. As the myotome grows it skews  
280 in the coronal plane (normal to the dorsoventral axis) such that the medial myotome is  
281 slightly anterior to the lateral myotome. Viewed from dorsal, the vertical myosepta on left  
282 and right sides form a broad chevron pointing anterior. If yaw is low, this morphology does  
283 not affect measurement of L. But if yaw is significant trigonometrical correction becomes  
284 challenging and a better approach is to measure True L directly by estimating the XYZ  
285 coordinates of the two points where the anterior and posterior vertical myosepta meet the  
286 notochord at the horizontal myoseptum. Simple trigonometry permits calculation of True  
287 L from these coordinates as  $L = \text{SQRT}[(X_2 - X_1)^2 + (Y_2 - Y_1)^2 + (Z_2 - Z_1)^2]$ . Weaknesses of  
288 this last approach are that a) selection of the points can vary with operator and b) no visual  
289 record of the points chosen is retained. This consideration does not affect CSA correction.

290  
291

## 292 5. Optional method: Remove and re-introduce muscle electrical activity

293  
294

295 5.1. At 3 dpf, split fish into three conditions: fish medium Control, Inactive and Inactive+Stim.  
296 1.3.1 For Inactive and Inactive+Stim groups, anaesthetise larvae at 9 am with Tricaine  
297 (0.6 mM). *NOTE:* Following <sup>38</sup>, frozen aliquots of tricaine stock are thawed and  
diluted (40  $\mu\text{l/ml}$  fish medium, to a final concentration of 0.6 mM) before adding to



298 fish. Do not add tricaine straight into the water containing fish, as some fish could  
299 receive high doses. Tricaine stock should be used within a month and never be re-  
300 frozen.

301 1.3.2 For the fish medium Control fish, leave them un-anaesthetised.

302 5.2. At selected time(s) after the onset of tricaine exposure (i.e. at 80 hpf), prepare the  
303 Inactive+Stim group for stimulation.

304 5.2.1. Create a stimulation chamber. Take a 6 × 35 mm-well plate, create two small  
305 openings (<5 mm in diameter) on each side of each well (see Figure 1) using a  
306 narrow soldering iron. *NOTE:* handle the hot soldering iron with care and work in a  
307 fume hood if desired to avoid inhaling vapour.

308 Thread a pair of silver or platinum wires (~20 cm-long) through the openings of each  
309 well (see Figure 1). Reusable adhesive material e.g. BluTack can be applied near  
310 the openings to keep the wires in place, and ensure a >1-cm separation between the  
311 wires (see Figure 1).

312 5.2.2. Prepare 60 mL of 2% agarose (1.2 g agarose powder in 60 mL fish medium), and  
313 melt fully using microwave, cool, add tricaine and pour 4 mL into each well of the  
314 stimulation chamber (Figure 1).

315 5.2.3. Immediately add custom-made 4-well combs in between the electrodes, (created  
316 by cutting out plastics e.g. polypropylene of desired dimensions and sticking together  
317 using Superglue; see Figure 1). Allow 10 min for gel to set. Remove combs carefully  
318 to create four rectangular wells.

319 5.2.4. Fill each well with tricaine water and place a single anaesthetised 'Inactive+Stim'  
320 larva in each well using a micropipette, with their anteroposterior axis perpendicular  
321 to the electrodes (see Figure 1).

322 5.2.5. Check under the dissecting fluorescent microscope that each fish is fully  
323 anaesthetised within each well of the chamber.

324 5.3. Connect an adjustable electrophysiological pattern-generating stimulator to the chamber  
325 via a Polarity Controller, using crocodile clips connected to each of the electrodes on one  
326 side of the chamber (see Figure 1). *NOTE:* The polarity controller is used to reverse the  
327 polarity every 5 seconds, so as to prevent electrolysis and corrosion of the electrodes.

328 5.4. Stimulate fish. For example, 1 s with a train of 200, 20 V pulses of alternating polarity,  
329 with 0.5 ms pulse duration and 4.5 ms pulse separation, once every 5 seconds gives an  
330 effective repeated-tetanic contraction 'resistance' regime.

331 5.5. Regularly check under the microscope that the fish are being stimulated; the example  
332 electrical stimulus should induce a visible bilateral contraction and slight movement, once  
333 every 5 seconds.

334 5.6. For a 'resistance/high force' regime, stimulate the fish for a bout of 5 mins, three times,  
335 with each bout separated by 5 mins of rest. *NOTE:* While fish on one side of the chamber  
336 are resting, the crocodile clips can be connected to the electrode pair on the other side  
337 of the chamber, and those additional fish stimulated.

338 5.7. After stimulation, carefully remove fish from each well by gently flushing them out with a  
339 plastic pipette and return to incubator in fresh tricaine-containing fish medium.

340 5.8. Pour away the tricaine water from within the chamber and use Forceps to cut around and  
341 remove the agarose from each well. Rinse the wells with tap water and allow to dry.

342 *NOTE:* If using silver wire electrodes, occasionally silver oxide may accumulate on the  
343 surface of the wire after a stimulation experiment. As silver oxide is less conductive than  
344 silver, to maintain reproducibility, careful rub silver oxide off the wire using Kimwipes  
345 before re-using the set-up.

346  
347  
348

349 **REPRESENTATIVE RESULTS:**

350

351 **A rapid and precise measure of somite volume**

352

353 A method of sample preparation, data acquisition and volumetric analysis that allows the rapid  
354 measurement of muscle growth in zebrafish larvae is described. Muscle size can be measured  
355 in live animals using fish labelled on their plasma membranes with a membrane-targeted GFP ( $\beta$ -  
356 *actin:HRAS-EGFP*) or mCherry ( $\alpha$ -*actin:mCherry-CAAX*). Larvae were transiently anaesthetised  
357 using tricaine, mounted in low-melting-point agarose and imaged using confocal fluorescence  
358 microscopy. Somite 17 was chosen for analysis of muscle size given its accessibility at the trunk-  
359 tail interface<sup>31</sup>. In practice, as in theory, myotome volume can be calculated as the product of  
360 myotome length (L) and the average of three cross-sectional area measures (CSA) (Figure 2A,  
361 which is referred to as the 4-slice method).

362

363 To validate this method, whole myotome confocal Z-stacks of live zebrafish larvae (Figure 2B)  
364 were obtained and somite volume was calculated by multiplying the sum of somite 17 profile areas  
365 in each slice (80-100 slices) by the inter-slice distance (1-1.2  $\mu$ m). A strong correlation was  
366 observed between the 4-slice and full stack methods of calculation (Figure 2C). However, the 4-  
367 slice method generally gave a slightly larger volume estimate (~2% larger on average) (Figure  
368 2D). This difference could be due either to a) obliquity of the samples giving erroneously large  
369 volume measurement or b) the observation that zebrafish myotomes taper along the  
370 anteroposterior axis, being smaller towards the tail of the animal. As the *YZa*, *YZm* and *YZp* CSA  
371 measurements are towards the anterior portion of the somite 17 myotome chevron (Figure 2A),  
372 the latter interpretation was tested by volumetric analysis of the myotomes of somites 16 and 18.  
373 Each somite was about 7% larger than the one behind (Figure 2E). Further analysis revealed  
374 that a '2-slice' method requiring only a single *YZ* measurement, located in the middle of the somite  
375 where the epaxial and hypaxial halves meet at the horizontal myoseptum (*YZm*), and the *XY* slice,  
376 gives a reasonably accurate estimate of myotome volume (Figure 2F,G). The 2-slice approach  
377 enables more rapid data acquisition when time constraints limit the number of fish that can be  
378 scanned. In summary, these data show that myotome volume can be measured rapidly and  
379 accurately in live zebrafish larvae. Single larvae were successfully repeatedly measured over a  
380 six day period with this method.

381

382 For comparative study of growth of an identified tissue unit, the described method provides  
383 reliable and precise volume estimates. To obtain accurate absolute volumes, however, a number  
384 of modifications can be applied. First, correction can be made for errors caused by oblique  
385 mounting either by tilting dish or microscope stage to obtain better transverse *YZ* and parasagittal  
386 *XY* slices during imaging or through using the notochord profile in *YZ* slices; the cross-sectional  
387 minor axis reveals the true diameter of the cylindrical notochord, whereas its major axis reveals  
388 the angle and magnitude of obliquity (see Note in point 4.5 above). Second, the location of *XY*  
389 and *YZ* sectioning during scanning must be selected to reflect accurately the desired myotome(s).  
390 (See Note in point 4.5 above). Note, however, that the form of the myotome chevrons changes  
391 depending on developmental stage and this must be taken into account when selecting *YZ* scans.  
392 Lastly, to determine if changes in myotome 17 reflect muscle growth throughout the axis,  
393 myotomes further into the trunk or tail regions may be measured by the described method.

394

395 **Repeated measurements reveal somite growth**

396

397 An advantage of the described method is the ease of repeated analysis on single fish. Individual  
398 embryos and larvae can be repeatedly embedded, measured and released without suffering

399 obvious long-term effects (Figure 2H). The myotome grows detectably both in L and CSA  
400 between 2 and 5 dpf, leading to steady increase in volume (Figure 2H). Growth was imaged in  
401 this way between 1 and 8 dpf and larvae were also released after imaging and grown to adulthood.  
402 Analyses further into the late larval period are expected to be possible, although effects of  
403 repeated imaging in feeding behaviour would need to be monitored carefully in comparison with  
404 siblings that are not imaged. Importantly, development of pigmentation can obscure imaging.  
405 Whereas pigmentation is not a problem in properly orientated fish, as the melanophore stripes do  
406 not prevent the required measurements, pigment is more problematic in obliquely mounted  
407 samples. The use of pigmentation mutant lines, such as *roy;mitfa*<sup>39</sup>, is anticipated, which would  
408 extend the time window of growth measurements until the limits of practicable confocal scan depth  
409 are reached.

410  
411 A further advantage of the described procedure is the ease of detailed analysis of growth of single  
412 fibres in comparison with their whole myotome over short periods. By mosaic labelling of fibres  
413 through DNA injection, a method was developed to detect nuclear acquisition and growth in  
414 individual identified fibres over four hours and then permit re-analysing at later times (Figure 2I).  
415 Moreover, growth of the whole myotome can be measured over 12 h or less<sup>26</sup> (and data not  
416 shown). By repeatedly measuring the same fish, inter-individual variability is eliminated and small  
417 numbers of animals can yield statistically robust results<sup>26</sup>.

418

#### 419 **Manipulations which change somite volume can readily be detected**

420  
421 The current protocol allows one to interrogate changes in muscle growth under various biological  
422 and physiological conditions, such as altered physical inactivity. Anaesthetic tricaine, which  
423 blocks nerve action potentials by inhibiting voltage-gated Na<sup>+</sup> channels<sup>40</sup>, was used to induce  
424 muscle inactivity in *β-actin:HRAS-EGFP* larvae. As shown previously<sup>26</sup>, inactivity for 24 h  
425 between the third and fourth dpf greatly reduced myotome volume, indicating that larval muscle  
426 growth is activity-dependent (Figure 3A). The effect of inactivity can also be investigated using  
427 other detection methods which reveal the structure of the somite, such as mCherry-CAAX (either  
428 in a transgenic line or by mRNA injection) or by overnight immersion of larvae in BODIPY dye  
429 (Figure 3A). The latter approach, while removing the need to cross fish onto transgenic  
430 backgrounds or inject embryos cannot be used for repeated measurements due to toxicity of  
431 BODIPY. Thus, the current method allows one reproducibly to measure changes in the volume  
432 of muscle tissue.

433

434 As described above, genetic marking methods can be used to make repeated measurements of  
435 myotome volume, permitting tracking of change in muscle size over successive days in individual  
436 fish. As individual fish and entire lays at the same development stage differ in absolute myotome  
437 volume (Figure 3A; perhaps due the size or health of eggs), the ability to measure growth of each  
438 individual reduces the effects of individual variation by permitting paired sample statistical  
439 analyses. Repeatedly measuring the same fish reduces the number of fish needed to detect  
440 effects robustly. To illustrate this effect, results from analysing the growth of each individual from  
441 3 to 4 dpf in populations of active and inactive larvae were compared with analysis of the same  
442 two populations using only the single measure of myotome size made at 4 dpf. From lay to lay,  
443 larger variation in apparent reduction of myotome size was observed when measuring myotome  
444 volume at 4 dpf only compared to measuring 4/3 dpf volume for each individual (Figure 3B). Note  
445 the greater range of reduction (68-91%) in the 4 dpf only measurements, compared to the 4/3 dpf  
446 method (78-89%) and the weak correlation between the two measures. Although, as expected,  
447 the mean reduction across all 13 biological replicates was similar in each assessment (Figure 3C)  
448 being  $82.62 \pm 1.01\%$  (mean  $\pm$  SEM, n=13) for the 4/3 dpf method and  $82.31 \pm 1.92\%$  for the 4 dpf  
449 only method, the estimated error with the 4 dpf only method was almost double that with the

450 4/3 dpf method. Thus, quantifying individual growth through repeated measurement is the more  
451 accurate method, by eliminating size variability between fish within the same lay, as demonstrated  
452 previously <sup>26</sup>. Nonetheless, as no significant difference in the reduction in myotome volume  
453 caused by inactivity was observed when measuring myotome volume at 4 dpf only (Figure 3C),  
454 the data suggest that ~6-8 fish are sufficient to average out inter-individual size difference within  
455 a lay. Clearly, when size changes are small the 4/3 dpf method is preferred.

456

457

### 458 **Analysis of the cellular basis of growth**

459

460 Myotome CSA is determined by muscle fibre number and fibre size. Fibre number can be  
461 estimated by counting the number of fast and slow fibres on three YZ sections (YZa, YZm, YZp).  
462 Although regions of two adjacent myotomes are contained in such YZ sections, as shown by the  
463 presence of vertical myosepta (VM) in most sections (Figure 2A), these counts accurately reflect  
464 fibre number. Over-counting occurs at VMs due to the tapering of pairs of fibres from each  
465 adjacent segment at the VM (Figure 4A). Such overcounting can be accounted for using the  
466 following equation: Fibre number = Total fibre count – (fibres in contact with VM)/2 ref <sup>33</sup>.  
467 Furthermore, average fibre volume can be determined by dividing myotome volume by the  
468 number of fibres. We have used these analyses to reveal that activity controls both cellular  
469 aspects of growth (Figure 4B,C).

470

471 It is evident from Figure 2A that fibres vary in size across the myotome, a reality that is not  
472 reflected in calculated average fibre volume measurements. By drawing around each fibre of  
473 somite 17 from two fish, measured fibre cross-sectional area was shown to range from 28  $\mu\text{m}^2$  to  
474 217  $\mu\text{m}^2$  (Figure 4D). In reality, however, many fibres are angled obliquely within the myotome,  
475 so such CSA measures do not reflect the true CSA of a fibre perpendicular to its long axis.  
476 Conversely, due to the varying angles of fibres within the myotome, all fibres running at  
477 orientations that are not aligned anteroposteriorly have lengths that differ from the myotome  
478 length. Despite these caveats, which can only be circumvented either by complete segmentation  
479 of the myotome into single fibre volumes or by calculation after measuring the angle of obliquity  
480 of each fibre, the measured CSAs provide an estimate of fibre size diversity in each fish. For  
481 example, individual fibres decreased in CSA with inactivity, resulting in a shift to the left in the  
482 cumulative frequency curve with respect to active (un-anaesthetised) control larvae (Figure 4E).  
483 As inactive fish have ~10 fewer fibres than active fish (Figure 4B), either the ten smallest fibres  
484 from active un-anaesthetised fish (on the assumption that they are the new ones) or the ten largest  
485 (as the alternative extreme) were omitted from the comparison, which showed that most loss of  
486 the myotome volume is due to lack of fibre growth, rather than failure of new fibre formation  
487 (Figure 4F). Taken together, these data show that the described method allows detailed  
488 investigation the role of physical activity on the formation and growth of muscle tissue.

489

### 490 **Reimposition of activity by electrical stimulation**

491

492 Physical activity is required for muscle growth (Figure 3A). A method to re-impose muscle  
493 contractions by electrical stimulation in otherwise inactive larvae, evoking a strong contractile  
494 response is described (Figure 5A, Supplemental File 8). Although precise stimulation parameters  
495 are described here (Figure 5B) to maximally activate the musculature, the protocol can be altered  
496 (by changing current amplitude, frequency, pulse duration etc) to control muscle activation and  
497 'exercise' dosage. Thus, the current method provides a controlled activity stimulus with  
498 standardised behaviour between activity bouts, overcoming an important limitation of current  
499 animal models of exercise <sup>18</sup>.

500

501 The described methods demonstrate the potential of using zebrafish larvae to study various  
502 aspects of muscle growth e.g. hyperplasia and hypertrophy. In particular, myogenesis in  
503 zebrafish larvae is shown to be amenable to analysis through pharmacologically-induced inactivity  
504 and electrically-induced contractility. The approach allows the study of the molecular  
505 mechanisms by which physical activity leads to muscle growth *in vivo*.

506  
507  
508

#### 509 **FIGURE AND TABLE LEGENDS:**

510

511 **Figure 1.** Design of a stimulation chamber for re-introduction of muscle electrical activity to  
512 zebrafish larvae. A six well cell culture plate fitted with electrodes permits maintenance of larvae  
513 in wells made within 2% agarose gel. Custom four-well combs are made to create rectangle wells  
514 (dimensions as indicated) in agarose to maintain position and orientation of individual fish larvae,  
515 and to prevent them from contacting the silver wires during vigorous twitching upon electrical  
516 stimulation.

517

518 **Figure 2.** Measuring muscle volume in live zebrafish  $\alpha$ -actin:mCherry-CAAX (A,B,E) or  $\beta$ -  
519 actin:HRAS-EGFP transgenic larvae. Larvae imaged from lateral view and shown dorsal to top,  
520 anterior to left in upper panels (A,B,E). **A.** In the 4-slice method, myotome volume was calculated  
521 by multiplying the length of somite 17 (L) measured between vertical myosepta (VM) on an XY  
522 plane (blue arrow) by the average of three cross-sectional areas (CSA) measured on YZ planes  
523 (YZm, YZa and YZp; dashed yellow lines). **B.** In the Full Stack method, the area of somite 17  
524 myotome was measured (examples outlined in yellow) in each slice of a whole Z-stack of a live  
525 zebrafish larva and the sum of myotomal areas was multiplied by the inter-slice distance. **C.** High  
526 concordance between the 4-slice and Full Stack methods. Colours denote individual  $\beta$ -actin:GFP  
527 (squares) or  $\alpha$ -actin:mCherry-CAAX (circles) fish. **D.** Myotome volume is slightly, but  
528 significantly, larger when calculated using the 4-slice method. **E.** In the tapering zebrafish larvae,  
529 more anterior somites are larger than posterior somites, as measured by the 4-slice method. **F,G.**  
530 Strong correlation between volume measurements made using the average of three CSA sections  
531 (4-slice method) or a single YZm CSA (2-slice method). *p*-values show results of two tailed t-  
532 tests with equal variance (D,G) or one way ANOVA with Bonferroni *post hoc* tests (E). ns, not  
533 significant. **H.** Measurement of myotome 16 volume, length (L) and cross-sectional area (CSA)  
534 from two to five dpf in three individual fish (colours) expressing  $\beta$ -actin:GFP and myog:H2B-  
535 mRFP. YZm images of the green individual at each timepoint are shown above. **I.** Single fibre  
536 growth measured by automated constant-threshold segmentation. A  $\beta$ -actin:HRAS-  
537 EGFP;myog:H2B-mRFP fish mosaically labelled by injection of a CMV:Cerulean plasmid at the  
538 1-2 cell stage. A single Cerulean marked fibre in somite 10 was scanned with high resolution full  
539 XYZ stacks repeatedly on a Zeiss LSM880. Images shown are representative single slices (left)  
540 and the projection of the three dimensional segmented volume (right). Each datapoint on the  
541 graph represents a single scan of the same fibre, at 3 dpf (0 h), after 4 hours, and at 5 dpf (54 h).  
542 Triplicate scans were made and segmented per time-point to show reproducibility. White  
543 arrowheads point to fibre nuclei; note that two nuclei are added between 3 and 5 dpf.

544

545 **Figure 3.** Activity-dependent muscle growth in somite 17. **A.** Inhibiting activity for 24 h by  
546 application of tricaine (pink) between 3 and 4 dpf reduces myotome volume both in transgenic  
547 lines and in non-transgenic fish stained with BODIPY compared to vehicle controls on siblings  
548 (blue). Volume quantified by 4-slice method. Symbol shape indicates replicate experiments from  
549 distinct lays (biological replicates). Large symbols denote mean  $\pm$  SEM values. Small faint  
550 symbols show the volume of individual replicate larvae. **B.** Comparison of myotome volume

551 reduction in inactive fish compared to control siblings determined by single measurement of  
552 myotome volume at 4 dpf (4 dpf only, upper schematic) or change in myotome volume between  
553 3 and 4 dpf (4/3 dpf, lower schematic). Each symbol represents the mean volume of myotome  
554 17 in ~5 inactive fish from a single lay divided by the mean myotome 17 volume of ~5 active  
555 control siblings. **C.** No difference was observed in the mean reduction in muscle growth in  
556 inactive fish, when measuring by the 4 dpf only or 4/3 dpf methods. Numbers within bars  
557 represent total number of fish analysed. *p*-values show results of two way ANOVA with Bonferroni  
558 *post hoc* tests (A) or two tailed t-test with unequal variance (C).  
559

560 **Figure 4.** Cellular level changes in muscle growth caused by inactivity. **A.** Schematic showing  
561 how overcounting occurs at VMs due to double counting of tapering fibers where the blue and red  
562 myotomes meet. Note that the average fibre count is 6 but the true mean value is 5.5. The  
563 corrected count gives a better approximation. **B,C** Fibre number (B) and average fibre volume  
564 (C) are reduced in inactive (pink) compared to active (blue) larvae. Symbol shape indicates  
565 replicate experiments from distinct lays (biological replicates). Large symbols denote mean  $\pm$   
566 SEM values. Smaller faint symbols show the value of individual replicate larvae. Numbers within  
567 bars represent total number of fish analysed. **D.** In single larvae, each fibre profile in myotome  
568 17 was outlined and CSA determined. Boxes show mean  $\pm$  SEM. *p*-values show results of two-  
569 way ANOVA with Bonferroni *post hoc* tests (B,C) or two tailed t-test with equal variance (D). **E,F.**  
570 Cumulative frequency curves showing fibre size distribution in active control (blue) and inactive  
571 (pink) larvae. Comparison of all fibres (E), or after omission of presumed-nascent small or, at  
572 the alternative extreme, large fibres (F) shows that fibre size increase, not increase in fibre  
573 number, primarily accounts for activity-driven growth of the myotome.  
574

575 **Figure 5.** Brief electrical stimulation evokes tetanic muscle contractions in anaesthetised zebrafish  
576 larvae. **A.** Sequential images (captured from video in Supplemental File 8) showing how electrical  
577 stimulation triggers maximal contractions of an anaesthetised larva at 3 dpf. Time scale in  
578 seconds. Red boxes indicate movements at start of three successive 1 s stimulation trains. Each  
579 image is a 40 ms exposure. **B.** Schematic showing the electrical stimulation regime, in which a  
580 1 s train of 200 high frequency, 20 V electrical impulses is given every 5 seconds.  
581

582 **Supplemental File 1.** Schematics of captured images of perfectly (top left) and imperfectly  
583 mounted larvae with respect to the microscope XYZ reference frame (black axes). Myotome  
584 (green), notochord (yellow), neural tube (tan), measured myotomal parameters (red), measured  
585 notochord parameters (black arrows) and possible or actual fish rotations (blue).  
586

587 **Supplemental File 2.** Screenshot showing somite length measurement from XY images in ZEN.  
588

589 **Supplemental File 3.** Screenshot showing CSA measurement from YZ images in ZEN.  
590

591 **Supplemental File 4.** Screenshot showing somite length measurement from XY images in  
592 Fiji/ImageJ.  
593

594 **Supplemental File 5.** Screenshot showing extraction of calibration parameters for YZ images  
595 from ZEN.  
596

597 **Supplemental File 6.** Screenshot showing calibration of YZ images in Fiji/ImageJ.  
598

599 **Supplemental File 7.** Screenshot showing CSA measurement from YZ images in Fiji/ImageJ.  
600

601 **Supplemental File 8.** Representative video showing muscle contraction evoked by direct

602 electrical stimulation (length 1 s) of a tricaine-anaesthetised 3 dpf larva.

603

604

605 **TABLE OF MATERIALS:**

606 See attached.

607

608

609 **DISCUSSION:**

610

611 Here we report a method for accurate and efficient estimation of the muscle volume of live  
612 zebrafish larvae at stages or in genetic variants in which pigmentation is not a big hinderance to  
613 imaging and when transient anaesthesia and/or immobilisation is well tolerated. Whereas we  
614 have employed laser scanning confocal microscopy, the approaches described are applicable to  
615 spinning disk confocal or light sheet microscopy and to any other method that creates stacks of  
616 images at distinct focal planes. A series of increasingly sophisticated approaches to tissue size  
617 and cell content estimation is described. Each method has advantages and limitations, which we  
618 show can be quantified. A major limitation in studying tissue growth is the difficulty of analysing  
619 growth changes in real time as growth rates alter in response to a series of molecular or sub-  
620 cellular events catalysed by acutely administered stimuli. Moreover, individual variation can  
621 create problems when separate individuals are compared. The current approach allows  
622 measurement of tissue growth over periods of less than a day in single live individuals.  
623 Application of the approach can be envisaged on the minute timescale.

624

625 The described methods permit analyses that were hitherto impracticable. Using the 4-slice  
626 method, the imaging portion of the muscle growth assay can be completed on a sample size of  
627 around 20 fish within an hour by a trained operator. This is in stark contrast to the conventional  
628 Full Stack method, which takes at least 3 hours for the same number of fish (i.e. three times  
629 longer). If high resolution images are required for subsequent sub-cellular analyses the Full Stack  
630 method can easily require 30 min per fish, making growth assays of cohorts of animals at a similar  
631 developmental stage impossible. In contrast, the 2- or 4-slice methods permit rapid high quality  
632 image capture. Moving to consideration of image analysis, the advantages of the 2- or 4-slice  
633 method in saving of operator time (in the absence of automated image segmentation) over the  
634 Full Stack method are enormous. Each fish requires about 20 min for Full Stack analysis, but  
635 only 3-4 min for 4-slice analysis. Operator time can be further conserved by using the almost-as-  
636 accurate 2-slice method. Thus, the described method is efficient and thereby increases flexibility  
637 in experimental design.

638

639 The major limitation of the 4- or 2-slice methods are their being estimates, due to the overlapping  
640 chevron shape of somites, of the volume of regions of two neighbouring somites e.g. in the  
641 examples shown, myotome 16 and 17. It is shown that this can over-estimate the actual myotome  
642 17 volume by around 2%, depending on precisely where YZ slices were selected. Moreover,  
643 manual tracing of the somite borders during measurements might contribute to variations in  
644 estimates, although little inter-experimenter difference was found (data not shown). Measurement  
645 errors might be addressed using thresholding, filtering, and segmentation algorithms to acquire  
646 surface area in a more objective and reproducible manner. However, customisations will still be  
647 required to account for variations in the background fluorescence (such as due to embedding  
648 and/or thickness of the LMA) and the expression level of fluorescence proteins of individual larva  
649 over time. Note that such automated measurements will be even more challenging if a non-  
650 muscle-specific reporter is used, such as the  $\beta$ -actin:HRAS-EGFP line. Nonetheless, under many

651 circumstances, for example when comparing effects of manipulations between fish subjected to  
652 different treatments that are expected to affect all muscle tissue, the inaccuracy may be  
653 immaterial. However, if maximal accuracy is required for comparison to fibre or nuclear numbers  
654 counted solely from myotome 17, for example, the 'slice' methods can be improved. This can be  
655 achieved either by using the arduous Full Stack method, by mathematical correction by  
656 multiplying the measured 4-slice volumes by 0.98, or by moving the location of the YZ CSA scans  
657 posteriorly to reflect more accurately the true CSA of myotome 17.

658  
659 A second limitation of the method is its sensitivity to the mounting orientation of the fish. In  
660 practice, skilled operators can orient fish within reasonable limits most of the time, even when  
661 working quickly to embed many samples. Modifications to equipment on the microscope stage  
662 can be envisaged that would allow correction of yaw and roll prior to scanning. Without such  
663 apparatus, a method to quantify misorientation that can then be used to correct the measured  
664 volumes is described. Moreover, even if misorientation increases variability in measured volume,  
665 and thus reduces the chance of observing small effect sizes, in many situations such variation  
666 will affect control and experimental samples similarly. So false positive results are unlikely, if  
667 operators are aware of the issue.

668  
669 The described methods have initially been applied to analyse the role of electrical activity in  
670 muscle growth, a subject with a long history of analysis in a wide range of species (reviewed in  
671 <sup>18</sup>). To this end, simple methods to block endogenously-triggered activity are described in detail  
672 and replaced with controlled patterned electrical stimulation in the zebrafish larva. Advantages  
673 of this approach are the removal of neural feedback controls <sup>40</sup>, the elimination of the effects of  
674 altered nutrition and the ability to analyse circadian effects on growth itself, rather than on growth  
675 proxies, such as protein turnover <sup>26</sup>. As different patterns of electrical activity, trigger distinct  
676 muscle responses, regulating fibre type, size and metabolism <sup>41-48</sup>, the current methods open the  
677 zebrafish to such analyses.

678  
679 The methods described offer a suite of techniques with which many aspects of muscle physiology,  
680 cell biology and pathology can be analysed in unprecedented temporal and spatial resolution by  
681 taking advantage of the relatively unexplored zebrafish. The current approaches could clearly be  
682 applied to other species, regions of the body, and developmental stages. The rapid early growth  
683 of zebrafish larvae makes detection of acute effects of manipulations on tissue growth and  
684 morphogenesis particularly attractive areas of study. Moreover, zebrafish muscle is shown to  
685 share various growth mechanisms and controls with mammals. While zebrafish are vertebrates  
686 that conserve many aspects of muscle molecular genetics, cell and developmental biology with  
687 humans, there are also significant differences in the control of muscle growth. For example, slow  
688 and fast fibre types are more clearly spatially segregated in fish and the innervation of muscle  
689 shows differences. Furthermore, it must be borne in mind that, so far, we have only been able to  
690 analyse the early stages of development. Similar analyses at later stages are envisaged.

691  
692

### 693 **ACKNOWLEDGMENTS:**

694 The authors are deeply indebted to the efforts of Hughes lab members Drs Seetharamaiah Attili,  
695 Jana Koth, Fernanda Bajanca, Victoria C. Williams, Yaniv Hinitz, Giorgia Bergamin and Vladimir  
696 Snetkov for development of the described protocols, and to Henry Roehl, Christina Hammond,  
697 David Langenau and Peter Currie for sharing plasmids or zebrafish lines. SMH is a Medical  
698 Research Council (MRC) Scientist with Programme Grant G1001029, MR/N021231/1 and  
699 MR/W001381/1 support. MA held a MRC Doctoral Training Programme PhD Studentship from  
700 King's College London. This work benefited from the trigonometrical input of David M. Robinson,



701 scholar, mentor and friend.  
702

703 **DISCLOSURES:**

704 The authors declare no competing interests.  
705

706 **REFERENCES:**

- 707
- 708 1 Hammond, J. A discussion on the measurement of growth and form; measuring growth  
709 in farm animals. *Proceedings of the Royal Society of London. Series B: Biological Sciences.*  
710 **137** (889), 452-461, (1950).
  - 711 2 Hubal, M. J. *et al.* Variability in muscle size and strength gain after unilateral resistance  
712 training. *Medicine and Science in Sports and Exercise.* **37** (6), 964-972, (2005).
  - 713 3 Stillwell, R. C., Dworkin, I., Shingleton, A. W. & Frankino, W. A. Experimental manipulation  
714 of body size to estimate morphological scaling relationships in *Drosophila*. *J Vis Exp.*  
715 10.3791/3162 (56), (2011).
  - 716 4 Gupta, B. P. & Rezai, P. Microfluidic Approaches for Manipulating, Imaging, and Screening  
717 *C. elegans*. *Micromachines (Basel).* **7** (7), (2016).
  - 718 5 Duckworth, J., Jager, T. & Ashauer, R. Automated, high-throughput measurement of size  
719 and growth curves of small organisms in well plates. *Scientific Reports.* **9** (1), 10, (2019).
  - 720 6 Erlandson, M. C., Lorbergs, A. L., Mathur, S. & Cheung, A. M. Muscle analysis using pQCT,  
721 DXA and MRI. *European Journal of Radiology.* **85** (8), 1505-1511, (2016).
  - 722 7 Buckinx, F. *et al.* Pitfalls in the measurement of muscle mass: a need for a reference  
723 standard. *Journal of Cachexia, Sarcopenia and Muscle.* **9** (2), 269-278, (2018).
  - 724 8 Haun, C. T. *et al.* A Critical Evaluation of the Biological Construct Skeletal Muscle  
725 Hypertrophy: Size Matters but So Does the Measurement. *Frontiers in Physiology.* **10**,  
726 (2019).
  - 727 9 Tavoian, D., Ampomah, K., Amano, S., Law, T. D. & Clark, B. C. Changes in DXA-derived  
728 lean mass and MRI-derived cross-sectional area of the thigh are modestly associated.  
729 *Scientific Reports.* **9** (1), 10028, (2019).
  - 730 10 Foessel, I. *et al.* Bone Phenotyping Approaches in Human, Mice and Zebrafish - Expert  
731 Overview of the EU Cost Action GEMSTONE ("GEnomics of MusculoSkeletal traits  
732 Translational Network"). *Frontiers in Endocrinology.* **12**, (2021).
  - 733 11 Epstein, H. F., Casey, D. L. & Ortiz, I. Myosin and Paramyosin of *Caenorhabditis-Elegans*  
734 Embryos Assemble into Nascent Structures Distinct from Thick Filaments and Multi-  
735 Filament Assemblages. *Journal of Cell Biology.* **122** (4), 845-858, (1993).
  - 736 12 Hresko, M. C., Williams, B. D. & Waterston, R. H. Assembly of body wall muscle and muscle  
737 cell attachment structures in *Caenorhabditis elegans*. *Journal of Cell Biology.* **124** (4), 491-  
738 506, (1994).
  - 739 13 Bao, Z. & Murray, J. I. Mounting *Caenorhabditis elegans* embryos for live imaging of  
740 embryogenesis. *Cold Spring Harbor Protocols.* **2011** (9), (2011).
  - 741 14 Schnorrenberg, S. *et al.* In vivo super-resolution RESOLFT microscopy of *Drosophila*  
742 *melanogaster*. *Elife.* **5**, (2016).
  - 743 15 Coquoz, S. *et al.* Label-free three-dimensional imaging of *Caenorhabditis elegans* with  
744 visible optical coherence microscopy. *PloS One.* **12** (7), (2017).

745 16 Laband, K., Lacroix, B., Edwards, F., Canman, J. C. & Dumont, J. Live imaging of *C. elegans*  
746 oocytes and early embryos. *Methods in Cell Biology*. **145** 217-236, (2018).

747 17 Pende, M. *et al.* High-resolution ultramicroscopy of the developing and adult nervous  
748 system in optically cleared *Drosophila melanogaster*. *Nature Communications*. **9**, (2018).

749 18 Attwaters, M. & Hughes, S. M. Cellular and molecular pathways controlling muscle size in  
750 response to exercise. *FEBS Journal*. 10.1111/febs.15820, (2021).

751 19 Morley, J. E. *et al.* Sarcopenia with limited mobility: an international consensus. *Journal*  
752 *of the American Medical Directors Association*. **12** (6), 403-409, (2011).

753 20 Bauer, J. *et al.* Sarcopenia: A Time for Action. An SCWD Position Paper. *Journal of*  
754 *Cachexia, Sarcopenia and Muscle*. **10** (5), 956-961, (2019).

755 21 Cruz-Jentoft, A. J. & Sayer, A. A. Sarcopenia. *Lancet*. **393** (10191), 2636-2646, (2019).

756 22 Knappe, S., Zammit, P. S. & Knight, R. D. A population of Pax7-expressing muscle  
757 progenitor cells show differential responses to muscle injury dependent on  
758 developmental stage and injury extent. *Frontiers in Aging Neuroscience*. **7**, (2015).

759 23 Gurevich, D. B. *et al.* Asymmetric division of clonal muscle stem cells coordinates muscle  
760 regeneration in vivo. *Science*. **353** (6295), aad9969, (2016).

761 24 Berberoglu, M. A. *et al.* Satellite-like cells contribute to pax7-dependent skeletal muscle  
762 repair in adult zebrafish. *Developmental Biology*. **424** (2), 162-180, (2017).

763 25 Ganassi, M. *et al.* Myogenin promotes myocyte fusion to balance fibre number and size.  
764 *Nature Communications*. **9** (1), 4232, (2018).

765 26 Kelu, J. J., Pipalia, T. G. & Hughes, S. M. Circadian regulation of muscle growth  
766 independent of locomotor activity. *Proceedings of the National Academy of Sciences of*  
767 *the United States of America*. **117** 31208-31218, (2020).

768 27 Currie, P. D. & Ingham, P. W. Induction of a specific muscle cell type by a hedgehog-like  
769 protein in zebrafish. *Nature*. **382** (1 AUG), 452-455, (1996).

770 28 Devoto, S. H., Melancon, E., Eisen, J. S. & Westerfield, M. Identification of separate slow  
771 and fast muscle precursor cells in vivo, prior to somite formation. *Development*. **122** 3371-  
772 3380, (1996).

773 29 Blagden, C. S., Currie, P. D., Ingham, P. W. & Hughes, S. M. Notochord induction of  
774 zebrafish slow muscle mediated by Sonic Hedgehog. *Genes & Development*. **11** (17), 2163-  
775 2175, (1997).

776 30 Du, S. J., Devoto, S. H., Westerfield, M. & Moon, R. T. Positive and negative regulation of  
777 muscle cell identity by members of the *hedgehog* and *TGF- $\beta$*  gene families. *Journal of Cell*  
778 *Biology*. **139** (1), 145-156, (1997).

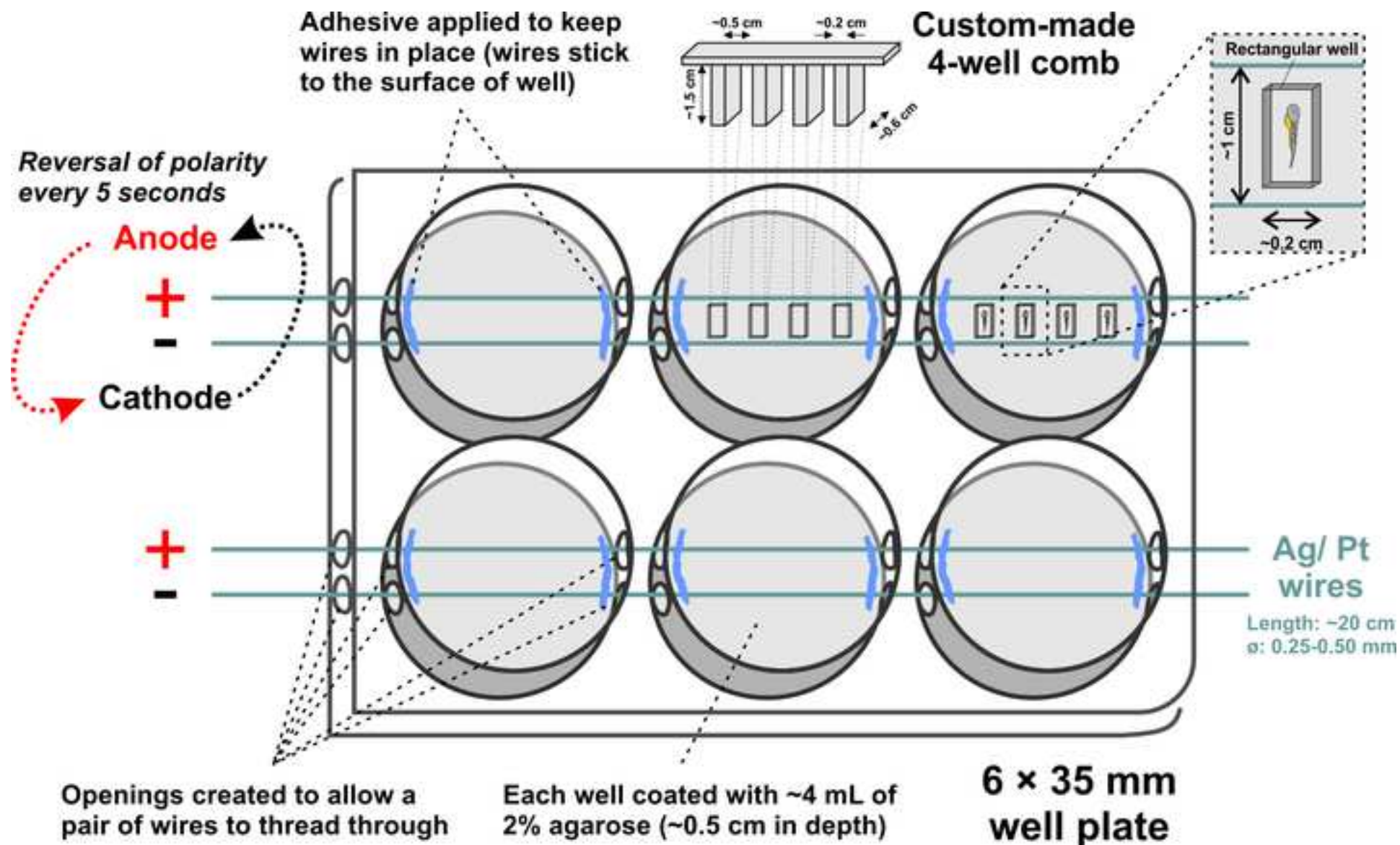
779 31 Hinitz, Y. *et al.* Defective cranial skeletal development, larval lethality and  
780 haploinsufficiency in Myod mutant zebrafish. *Developmental Biology*. **358** (1), 102-112,  
781 (2011).

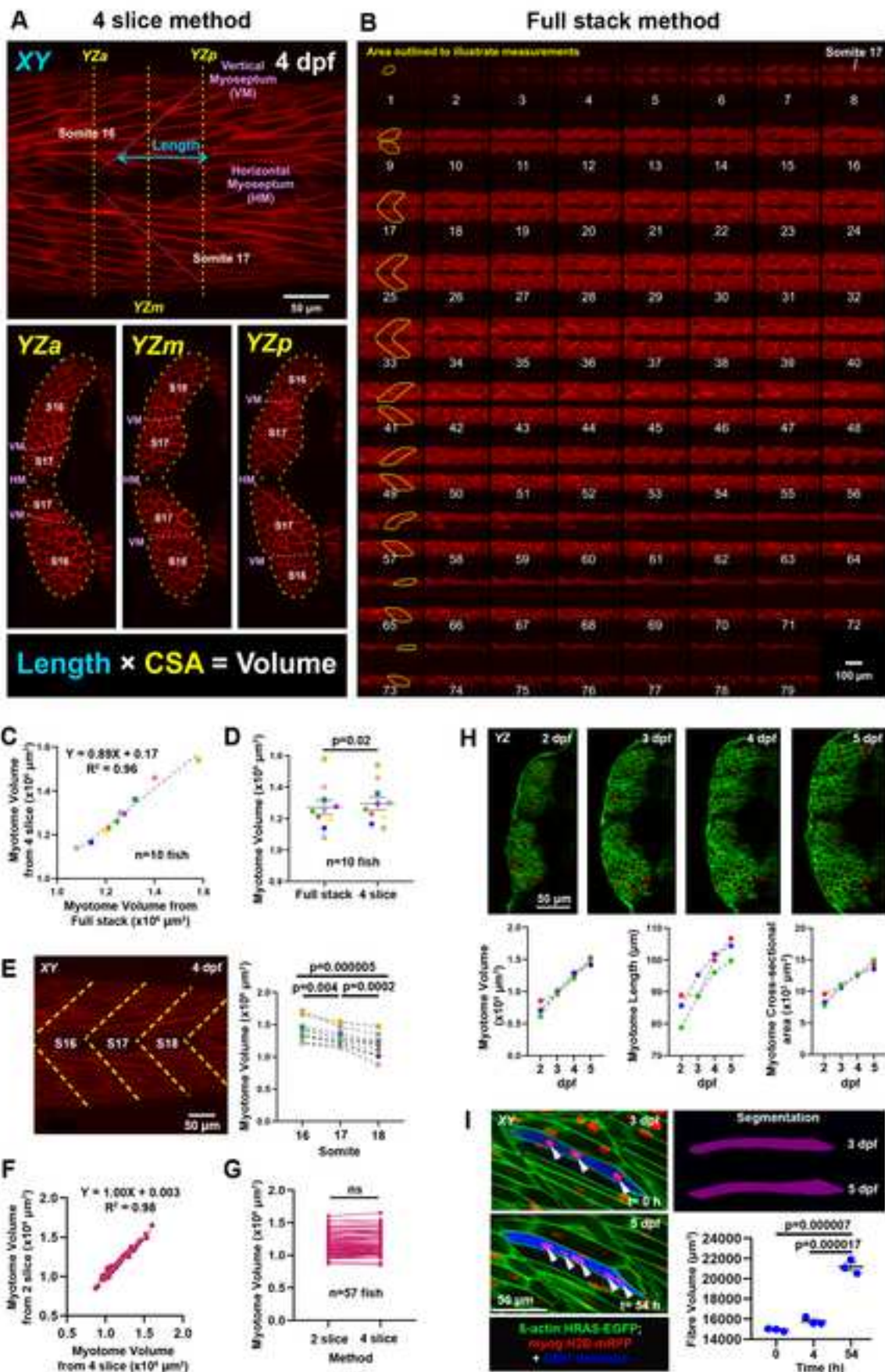
782 32 Pipalia, T. G. *et al.* Cellular dynamics of regeneration reveals role of two distinct Pax7 stem  
783 cell populations in larval zebrafish muscle repair. *Disease Models & Mechanisms*. **9** (6),  
784 671-684, (2016).

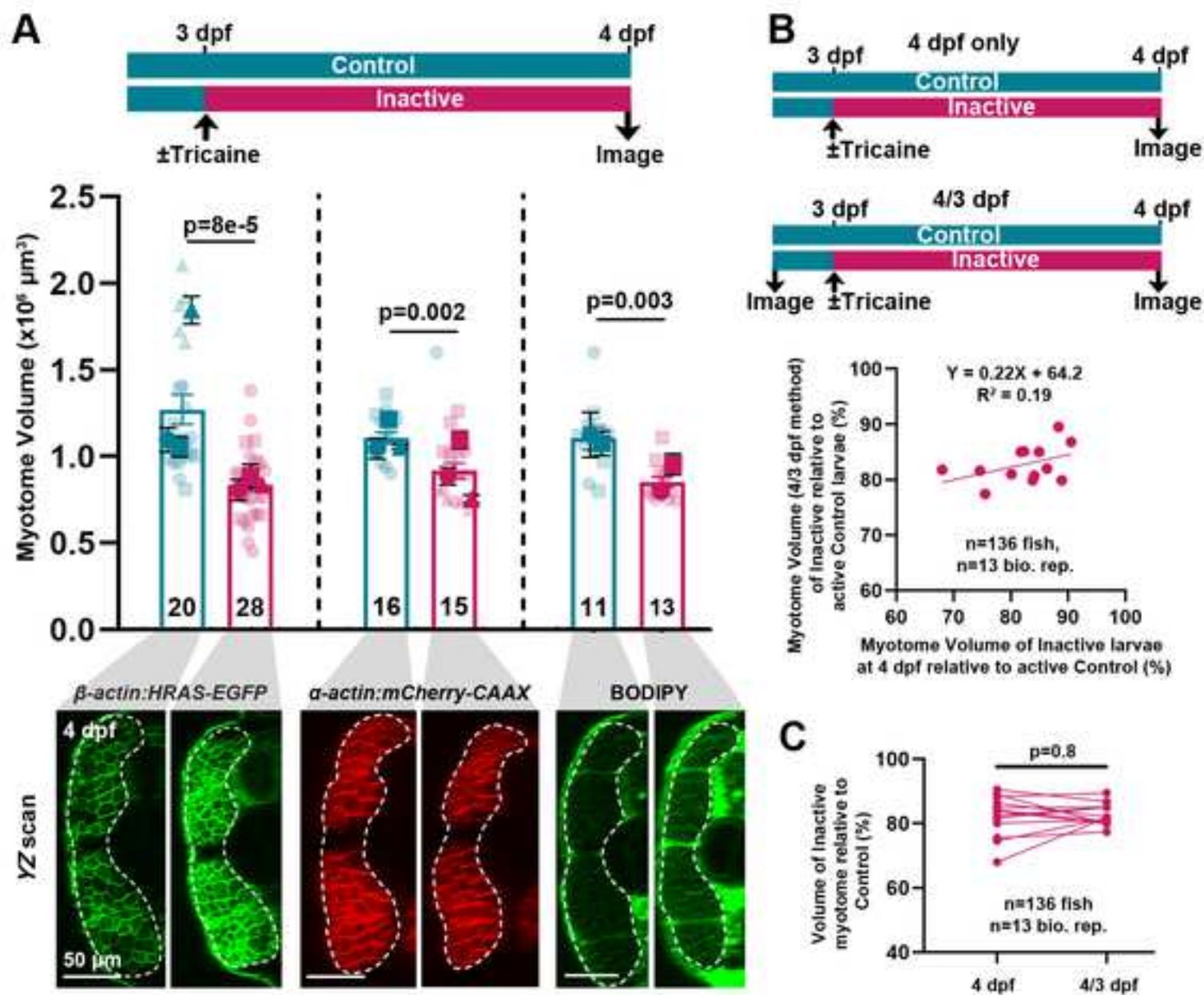
785 33 Roy, S. D. *et al.* Myotome adaptability confers developmental robustness to somitic  
786 myogenesis in response to fibre number alteration. *Developmental Biology*. **431** (2), 321-  
787 335, (2017).

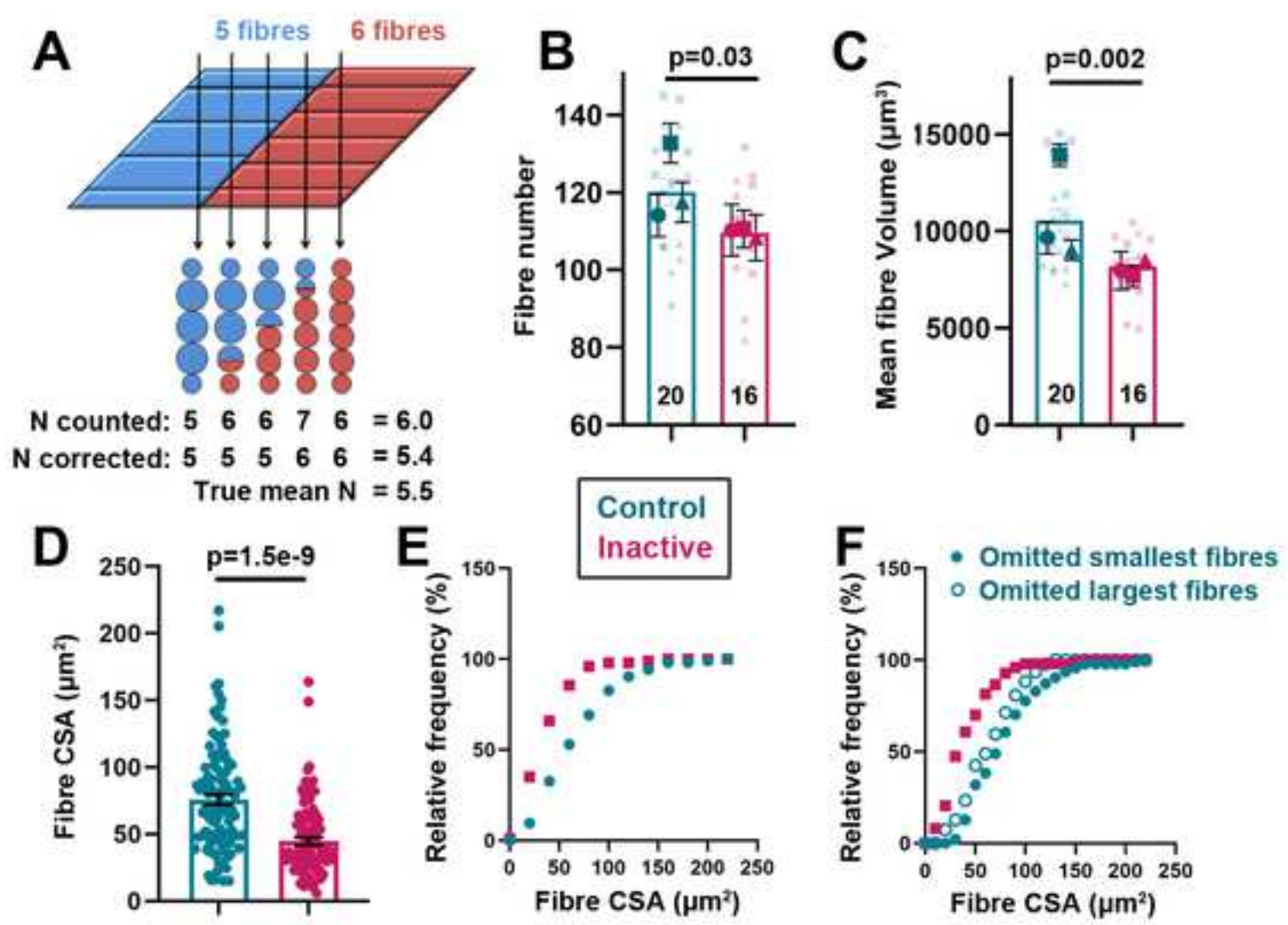
788 34 Zhang, W. & Roy, S. Myomaker is required for the fusion of fast-twitch myocytes in the

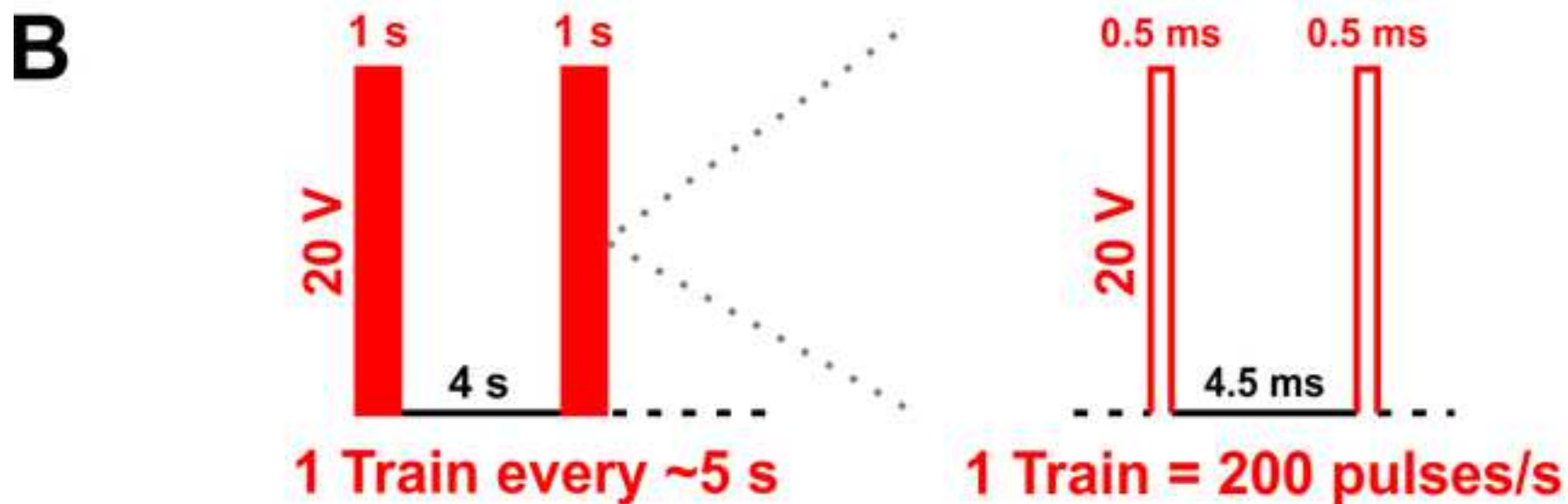
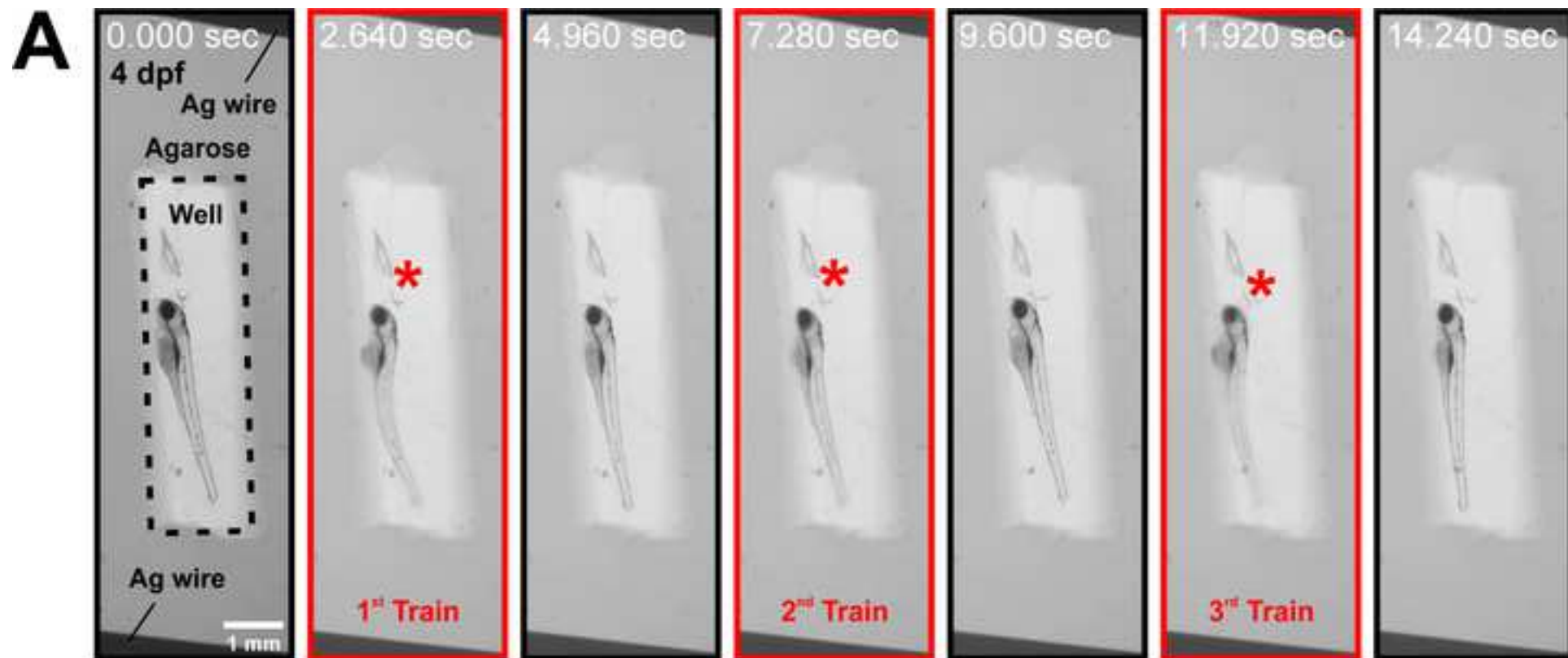
789 zebrafish embryo. *Developmental Biology*. **423** (1), 24-33, (2017).  
790 35 Osborn, D. P. S. *et al.* Fgf-driven Tbx protein activities directly induce myf5 and myod to  
791 initiate zebrafish myogenesis. *Development*. **147** (8), dev184689, (2020).  
792 36 Cooper, M. S. *et al.* Visualizing morphogenesis in transgenic zebrafish embryos using  
793 BODIPY TR methyl ester dye as a vital counterstain for GFP. *Developmental Dynamics*. **232**  
794 (2), 359-368, (2005).  
795 37 Berger, J., Hall, T. E. & Currie, P. D. Novel transgenic lines to label sarcolemma and  
796 myofibrils of the musculature. *Zebrafish*. **12** (1), 124-125, (2015).  
797 38 Westerfield, M. *The Zebrafish Book - A guide for the laboratory use of zebrafish (Danio*  
798 *rerio)*. (University of Oregon Press, 2000).  
799 39 White, R. M. *et al.* Transparent adult zebrafish as a tool for in vivo transplantation analysis.  
800 *Cell Stem Cell*. **2** (2), 183-189, (2008).  
801 40 Attili, S. & Hughes, S. M. Anaesthetic tricaine acts preferentially on neural voltage-gated  
802 sodium channels and fails to block directly evoked muscle contraction. *PloS One*. **9** (8),  
803 e103751, (2014).  
804 41 Theriault, R., Boulay, M. R., Theriault, G. & Simoneau, J. A. Electrical stimulation-induced  
805 changes in performance and fiber type proportion of human knee extensor muscles.  
806 *European Journal of Applied Physiology*. **74** (4), 311-317, (1996).  
807 42 Roy, D., Johannsson, E., Bonen, A. & Marette, A. Electrical stimulation induces fiber type-  
808 specific translocation of GLUT-4 to T tubules in skeletal muscle. *American Journal of*  
809 *Physiology-Endocrinology and Metabolism*. **273** (4), E688-E694, (1997).  
810 43 Perez, M. *et al.* Effects of transcutaneous short-term electrical stimulation on M. vastus  
811 lateralis characteristics of healthy young men. *Pflugers Archiv-European Journal of*  
812 *Physiology*. **443** (5-6), 866-874, (2002).  
813 44 Boncompagni, S. *et al.* Structural differentiation of skeletal muscle fibers in the absence  
814 of innervation in humans. *Proceedings of the National Academy of Sciences of the United*  
815 *States of America*. **104** (49), 19339-19344, (2007).  
816 45 Gundersen, K. Excitation-transcription coupling in skeletal muscle: the molecular  
817 pathways of exercise. *Biological Reviews of the Cambridge Philosophical Society*. **86** (3),  
818 564-600, (2011).  
819 46 Egan, B. & Zierath, J. R. Exercise Metabolism and the Molecular Regulation of Skeletal  
820 Muscle Adaptation. *Cell Metabolism*. **17** (2), 162-184, (2013).  
821 47 Sillen, M. J. H., Franssen, F. M. E., Gosker, H. R., Wouters, E. F. M. & Spruit, M. A. Metabolic  
822 and Structural Changes in Lower-Limb Skeletal Muscle Following Neuromuscular Electrical  
823 Stimulation: A Systematic Review. *PloS One*. **8** (9), (2013).  
824 48 Khodabukus, A. *et al.* Electrical stimulation increases hypertrophy and metabolic flux in  
825 tissue-engineered human skeletal muscle. *Biomaterials*. **198** 259-269, (2019).  
826













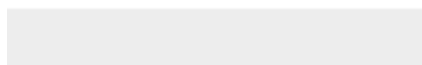
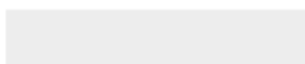


Click here to access/download  
**Video or Animated Figure**  
Supplemental File 8.avi





Click here to access/download  
**Table of Materials**  
JoVE\_Materials\_v10.xlsx



Dear JoVE

Thanks for the extensive Reviewer comments which have helped to improve significantly our presentation. We have removed some data (Figs 5 and 6), as suggested by Reviewer 3, but have retained our methodology for imposing both loss and gain of function of electrical activity on zebrafish larvae as we believe this is a powerful method for understanding neuromuscular growth control.

Thanks for your consideration of our revised manuscript.

Best wishes, Simon

**Reviewer #1:**

Manuscript Summary:

The authors describe and compare several approaches to zebrafish larval muscle measurement using confocal imaging. Technical details of image acquisition and analysis are given, along with instructions how to avoid potential caveats. The authors further expand on the subject by including an experiment with inactive and stimulated larvae, as a demonstration of the protocol efficacy. The manuscript could be of potential use to researchers coming into the field of zebrafish muscle biology. The manuscript is well written, although some parts could be revised to improve readability (particularly the several longer sentences in the introduction). However, certain issues need clarification before publishing.

Major Concerns:

The title is not entirely appropriate. Although the authors did perform live imaging, the experiments did not actually require "real time" readout, as imaging on several timepoints was sufficient. Furthermore, in order to observe muscle growth in real time, which was not the case here, more challenges would have to be addressed (heating bed/chamber, effect of immobilisation/anaesthesia on muscle development etc.).

**The Reviewer makes a good point. We have now added two kinds of data (in part in response to Reviewer 3) showing a) repeated measures over many days in the same fish (Fig. 2H) and growth of a single fibre over 4 hours in a continuous timelapse session (Fig. 2I). The Reviewer is correct that use of anaesthetic during embedding will slow growth (as we showed in our Kelu et al 2020 PNAS paper) but in the current analysis, after brief anaesthesia during embedding, one can then remove the tricaine and keep the fish embedded. 'Real time' for growth does not need to be on the second timescale, but more like the hour. This is achievable, as we show.**

Line 223 - 224: Differences in estimates mentioned here can also be attributed to manual drawing of muscle borders. A more reproducible results can be obtained by combining filters (such as median) and segmentation algorithms to acquire surface area. This would work well with muscle cell-specific reporter lines, but could be problematic if the reporter is more widely expressed. Authors should reflect on this issue.

**Good point. We have now included discussion of this issue at Ln 642-650.**

Line 229-231: In case of yaw (rotation around D-V axis), myotome length can only be underestimated, as its projection on the xy plane (in which you measure) would be shorter.

**This was also our initial thinking, but it is not correct. When one takes an XY plane photo of a fish embedded with yaw, one is taking a photo of a real plane at an angle through the myotome. One is not observing a projection of the myosepta from the 'desired' perfectly aligned plane (a parasagittal section) onto the XY plane of the microscope. Thus, the distance between the two myosepta can only be elongated (in exactly the same way as, in the YZ plane, the notochord becomes elongated in the direction of the major axis but retains its true diameter in the orthogonal minor axis, a phenomenon many people find easier to visualize). No line between two myosepta can ever be shorter than a line normal to the plane of those myosepta, and thus**

**a correction to correct L for its artificial elongation is required, as we describe.**

Lines 238-244: Would it be more appropriate to call it "Corrected/Adjusted" CSA rather than "True"? This part would be much clearer if accompanied by an additional illustration.

**Good idea. We now include such an illustration (new Supplemental File 1) and further explanation, as the rationale is not always obvious, as illustrated by the confusion on the previous point.**

Minor

Concerns:

Line 121: Authors should emphasise they are using an upright microscope. Working with an inverted setup would require a slightly different approach.

**This is true. We now mention it at In 149-155.**

Line 128: Authors should describe this step in more details. Which tools to use? Micropipette, Pasteur pipette? Should care be taken not to dilute the agarose further in the process... This is an important and delicate step. Inexperienced experimenters might encounter difficulties here.

**We have done as suggested.**

Lines 386-392: Authors discuss estimating fibre number by using YZ sections parallel to dorsoventral axis. What about using sections in YZ plane parallel to the VM? This way only fibres from myotome 17 would be counted. If authors have a Z-stack of myotome 17, they could use the "reslice" option in ImageJ/Fiji (use line tool to define the plane angle) to obtain these kind of "optical sections" and count the cells. If a membrane marker is used, one should be able to count individual cells despite the fact that the cross-sections appear slightly skewed. This would have to be done separately for dorsal and ventral muscle mass, sacrificing speed. But it would be interesting to compare fibre number obtained in this way to the authors estimate.

**These things are all true. It seems we failed to make clear that a big advantage of our method is that many individual fish can be analysed in a single experiment. It is precisely to avoid having to capture entire stacks (which slows both imaging and analysis markedly unless one has access to some unusually fancy kit) that we developed our methods, which can be employed on even a basic LSM confocal.**

Figures 5 and 6: Yellow colour on white background (and vice versa) is hard to read due to lack of contrast. I suggest using different colour here.

**We have now deleted these Figures.**

**Reviewer #2:**

Manuscript Summary:

The title and abstract are appropriate and should attract interest of researchers using zebrafish to model muscular dystrophies or mechanisms of skeletal muscle development. It could possibly be of used to also investigate interactions of muscle with nervous system where motor neuron innervation might be visualised and assessed using this method by scientists modelling motor neuron disease, using additional transgenic lines.

The materials and equipment needed listed is complete and the protocol steps are clearly and fully explained. More detail on controls is not required as the application maybe used in conjunction with different approaches (genetic/ gene targeting/drug treatment) each would need different consideration of appropriate controls. It is good that the authors have highlighted the critical steps; this is very important when using a new protocol.

The results shown are really beautiful and the extraction of such useful data from beautiful images is great. Being able to measure and calculate differences in muscle growth will be useful to researchers in the field of developmental biology and medical research. The range of references included is good.

Major Concerns:

None

Minor Concerns:

None

**Reviewer #3:**

Manuscript Summary:

The article "Real time measurement of skeletal muscle growth in live zebrafish" by Attwaters et al, describes an imaging based technique to examine myotome volume in zebrafish, and potentially examine growth stretches such as hypertrophy and hyperplasia. This topic is of great importance, and I clearly see merit in publishing this protocol in Jove. Although the technique is very simple, I think the authors have identified the various challenges faced in examining muscle growth in zebrafish, and importantly have performed detailed validation/optimisation which has addressed potential flaws of the technique.

Major Concerns:

However, I strongly feel that in its current form, the manuscript is more suited for a research article and not written appropriately for JOVE, which is focused on sharing cutting-edge experiments enabling efficient learning and replication of new research methods and technologies. The manuscript has too much scientific data which although is interesting, it is complex, difficult to read and follow, and importantly, the methodology in question seems to be diluted. For example, the authors need to consider if the electric activity protocol is really required in this study? To me, it seems like a cool protocol to stimulate the muscle activity but it does not provide a way to examine growth - which is the goal of the protocol. In line with this, I strongly feel that Figures 5 and 6 (and all related text) can be omitted as they do not necessarily demonstrate validity of the protocol. This will make the protocol and all the optimisation experiments (Figures 1-4) a lot clearer to understand and follow.

**While we are gratified that the Reviewer finds our method has merit, we think that a simple demonstration of the ability to combine the growth assay with manipulations that alter growth is in the spirit of the section entitled 'Representative Results'. The data included in no way constitute a meaningful and informative study for the primary research literature. Nevertheless, we take the Reviewer's point, so we have now made three significant changes to the data presented:**

- 1. We have added further characterisation of the timecourse of growth in Fig. 2H and I, as requested by Reviewer 1.**
- 2. We have removed the RNAseq data (Fig. 5)**
- 3. We have removed the stimulated growth data (Fig. 6). However, we think retention of the detailed description of the stimulation apparatus and method is desirable in a JoVE video context. Such a full description would not be possible, or easily discoverable, in more focussed research paper/s. So we have replaced Figs 5 and 6 with a new Fig 5 showing how the stimulation of the fish triggers movement.**

Abstract needs to be rewritten to clearly describe the focus of the protocol. As it is written, it is very difficult to follow what the article is about.

**We have now refocused the Abstract as suggested.**

Up until the discussion section, it is not clear what the goal/aim of step 5 "Optional method: Remove and re-introduce muscle electrical activity" is. This needs to be clarified early on, perhaps when step 5 is listed. Given that it is not really a protocol for examining growth, consider removing this part from the protocol.

**We prefer to retain the protocol, but we have now re-written the Abstract and also included altered electrical activity in the title to highlight that this is also described.**

It is unclear why a Z stack is set up (step 3.3) but after this only snap images of says that a Z-Stack is set up, steps 3.4 and 3.5 suggest that only 2 dimensional images are captured. Is this correct, and if yes, please justify why this is the case (apart from saving time?).

**We now explain more clearly that it is indeed to save time, as measuring many larvae is the key to robust statistical analysis. On a Zeiss scope (with ZEN software) it is necessary to define a stack in order to obtain a YZ slice image of the desired dimensions.**

How exactly are the YZ slices determined to ensure consistency between each fish? With the way the protocol is currently written, it appears that the YZ slices are selected without any real measure and are quite subjective. This of course can be different for each fish, and as such, it would be better to have a more definitive way of defining each YZ slice.

**Thanks for pointing out this serious omission. We are indeed careful about reproducibility in this respect, and have now explained precisely the issues and how they should be resolved in the text at ln 188-200.**

As shown by the investigators, different somites can have significantly different volumes and potentially growth dynamics. As such, while I appreciate that it is not possible to examine the entire trunk of the fish, perhaps, it is better to examine at least 3 neighbouring myotomes rather than just relying on a single one?

**Good point. As illustrated, we have done some of this, and we now make the issue clear at ln 370-373 and in Fig. 2E.**

Line 333: "We have successfully measured single larvae daily for over 5 days with this method". Was the same fish followed over a 5 day period? If yes, please include this data and include images to show comparison of growth of the same myotome at each day? This will significantly strengthen the paper and demonstrate the power of the approach.

**We have now included daily somite volume data from three fish between 2 and 5 dpf in Fig. 2H and discussed what further extension may be possible in ln 397-409. In addition, we have added new relevant data in Fig. 2I.**

Figure 3A: While the graph clearly demonstrates that inactivity reduces myotome volume, representative images of control and tricaine fish are needed to show what the myotome looks like in each case - rather than just of the control fish. The authors may choose to do this for each of the 3 strategies they have used - HRA-eGFP, mcherry-CAAX, and Bopidy.

**We now include such images in Fig. 3A.**

Figure 3B: It is not exactly clear what the graph represents and how these calculations have been made. Have the authors examined the same fish at 3 days, before addition of tricaine, and then again at 4 days (after approximately 24 hours of tricaine). If this is the case, please provide more explanation of what exactly was done, and what the graphs represent. The low R2 value suggests that there is weak correlation between the 4 dpf and 4/3 method but this does not support the usability of one approach over the other. The more detailed explanation should help clear this up.

**Thanks for pointing the lack of clarity out. We have now expanded the description to explain why (and how) the 4/3 dpf method is demonstrated to be superior (if more time-consuming) to the 4 dpf only method in ln 434-455.**

Line 409: "As inactive fish have ~10 fewer fibres than active fish (Figure 4B), we also omitted from the comparison the ten smallest fibres from active un-anaesthetized fish (on the assumption that they are the new ones)" which showed that most loss of the myotome volume is due to fibre shrinkage, rather than failure of new fibre formation." This seems like a circular argument and without more data whereby the identity and lineage of a cell is followed before and after tricaine, the conclusion that "most loss of the myotome volume is due to fibre shrinkage" is unwarranted. Given that the aim of this manuscript is to provide a detailed protocol on how to examine growth, rather than identify mechanisms of growth, I strongly feel that this statement needs to be removed. Only data pertaining to the validity of the protocol needs to be included, and this data (4E and 4F) doesn't do that. It in fact, leaves the reader with more questions than answers.

**We disagree with the Reviewer; it is in no way a circular argument. We think it important to alert readers to the potential pitfalls in growth analyses, and this is one of them. By including this analysis (it is not extra data *per se*) we show how to deal logically with the issue of distinguishing growth due to new fibre formation from that due to fibre expansion. We omitted the smallest fibres in our calculation because this is likely to reflect reality: new fibres are small. However, if we instead omit the ten largest fibres (a very unlikely scenario: that the largest fibres are the most recently-formed ones and are missing in inactive fish), we now show in the revised Fig. 4F that the reduction in fibre CSA of the residual fibres still makes a large contribution to the reduction in muscle mass.**

Figure 5: It is unclear how the protocol described permits the study of molecular mechanisms. The protocol described allows the examination of myotome volume and does not reveal any molecular changes. Please delete this data and if you choose to include it, please amend the protocol appropriately.

**Now deleted.**

Figure 6: Again, this data seems unnecessary and seems more appropriate for a research article rather than for JOVE, which is geared to sharing protocols rather than scientific data.

**Now deleted as requested, and instead illustrative data of how the stimulation protocol triggers movement is included.**

Minor Concerns:

Line 26: "A further protocol is described that controls muscle contractile activity". This does not make sense

**The Abstract has now been significantly altered and this sentence clarified'.**

4.4.1 - Please elaborate what the authors mean by "correctly calibrated". Is scale?

**Now explained.**

Line 320: "observed between both methods of calculation". Given that the 4-slice method is discussed in the next statement, it is not clear what "both" is referred to here.

**Clarified.**

Line 50. Change advance to advances

**Done.**

Please add discussion on hypertrophic and hyperplastic growth in the introduction, as the technique described clearly has the potential of addressing this.

**We have now added this to the Introduction.**

What is the maximum age of fish that this technique can be used on - given the obvious challenges faced in imaging larger fish? Please add this as a limitation.

**Good question. Now addressed in ln 402-409. We have done this on 8 dpf larvae and anticipate it could be used much later in fish carrying pigmentation mutations, such as *roy;mtifa*.**

**Reviewer #4:**

Manuscript Summary:

In this study the investigators developed an effective approach to analyze live fish embryonic and

larval muscle growth using confocal laser scanning microscopy to visualize muscle fibers with fluorescently marked plasma membranes. By using the approach, they demonstrated that muscle inactivity dramatically reduced muscle growth. The reduced muscle growth was largely rescued by a brief electrical stimulation. Overall, this was a well-designed and executed studies. The data are of high quality and support the conclusions. The described methods provide a powerful tool to study the effect of genetic, drug or environmental factors on a variety of cellular and physiological muscle growth parameters in living organism. A few minor comments may help clarify potential questions from future users.

Minor Concerns:

1. In Fig. 2A, it appears that slow fibers in the horizontal myoseptum were not clearly labeled by a-actin:mCherry-CAAX. Is this true? Any explanation?

**This is due to the presence of pigment cells in the horizontal myoseptum in the fish shown.**

2. In Fig. 6 the investigators showed that a brief electrical stimulation could rescue the growth reduction caused by 24 h of inactivity. Was this due to increased CSA or numbers of myofibers or both?

**At the request of Reviewer 3, we have now removed this data from the manuscript.**

3. All studies were performed on 3-4 dpf fish larvae. Could this method be used analyze myofibers in older fish larvae?

**Good point. We now show a time course study in Fig 2H and discuss this issue at ln 397-409.**

**Reviewer #5:**

Manuscript Summary:

The authors describe a live imaging protocol of skeletal muscle cells in zebrafish larvae. This detailed protocol includes procedures for sample preparation, data acquisition, and volumetric analysis. The muscle cell size can be measured very elegantly using a transgenic fluorescent report that target plasma membranes. The author thoughtfully provided methods and discussions to correct the over-counting of fiber numbers due to the presence of vertical myosepta and obliquity within the myotome. One potential problem of live-imaging muscle growth is that inactivity will affect the growth. They demonstrated that an electrical stimulation can maintain the growth of skeletal muscle. The manuscript is very well-written and the data are of high quality. Due to some of the caveats, the authors have to make a few assumptions in their measurement. Nonetheless, the manuscript has demonstrated a feasible protocol of live imaging of zebrafish skeletal muscle cells in larvae.

Major Concerns:

NA

Minor Concerns:

1. Please clarify the concentration of the agarose. It is 1% in the text and 2% in Figure 1.

**Thanks for noticing this. We have now clarified, in Fig. 1 the 2% agarose is used to make water-filled chambers to maintain the orientation of the larvae in the stimulation electric field, not for embedding. In the text, by contrast, we describe embedding in 1% low melt agarose for confocal scanning.**

2. The authors mention that this protocol is well-tolerated for zebrafish larvae. Can the fish larvae be recovered after imaging and continue to grow? The authors might comment on this since it will be very helpful if the larvae can be recovered and perhaps analyzed at later stage.

**Good point. Yes. We now show a time course study in Fig 2H and discuss this issue at ln 397-409.**

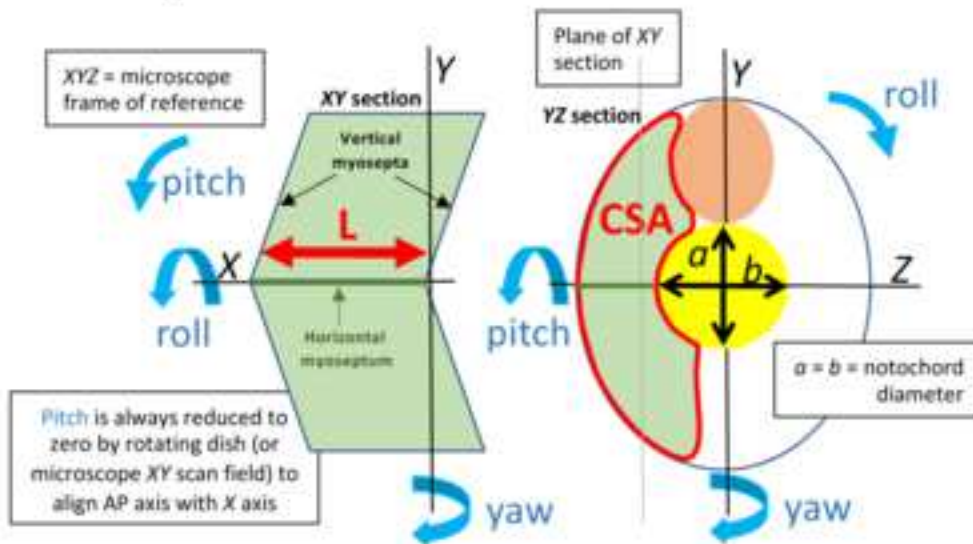
3. General writing suggestions- The authors should consider to keep the description of each step (for



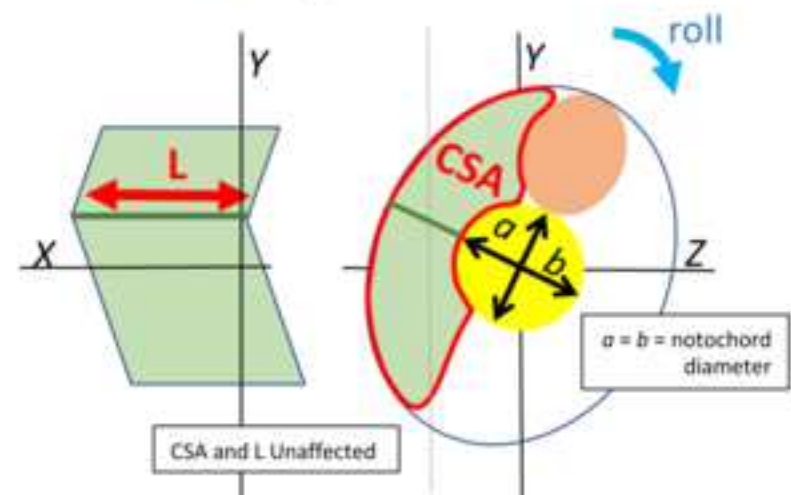
instance 3.4, 3.5, 4.2, 4.4.) succinct. This will be easier for the readers to follow the protocol. Some of the descriptions might be incorporated into representative results.

**We have tried to abbreviate where possible.**

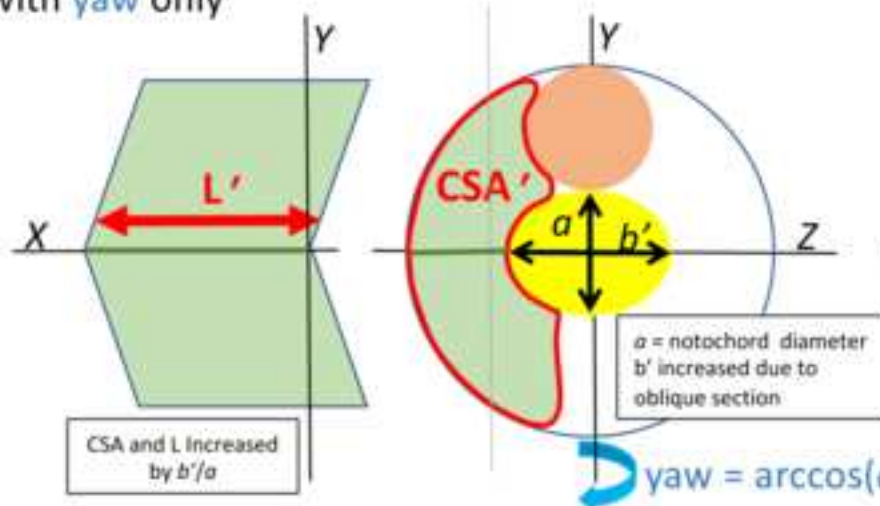
## Perfectly orientated fish



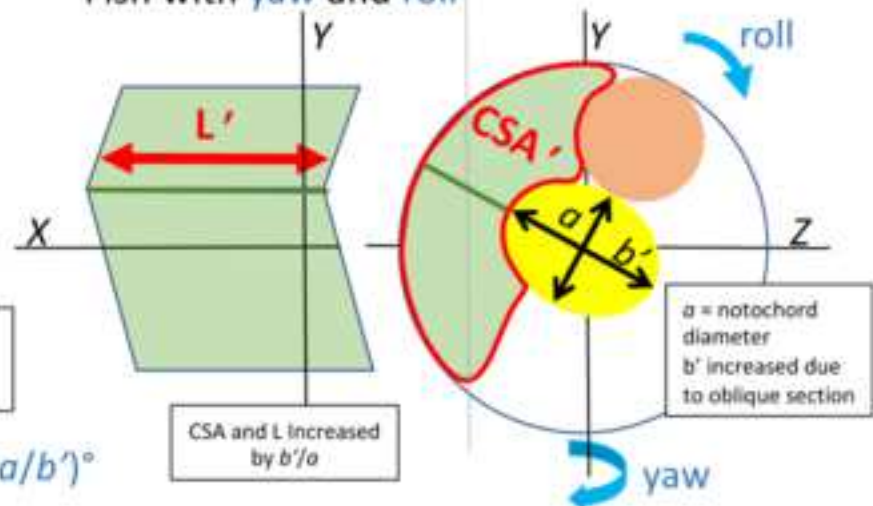
## Fish with roll only

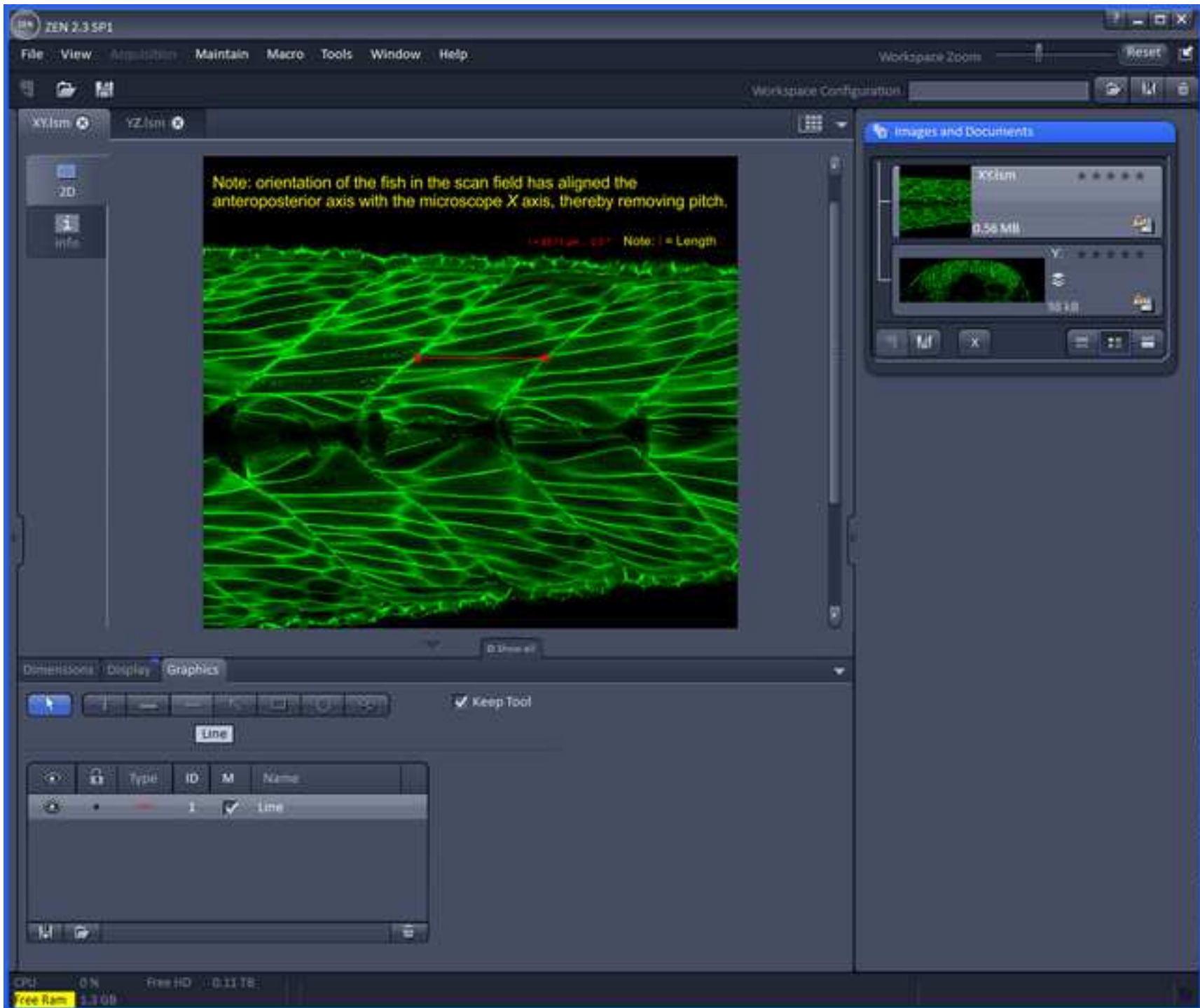


## Fish with yaw only

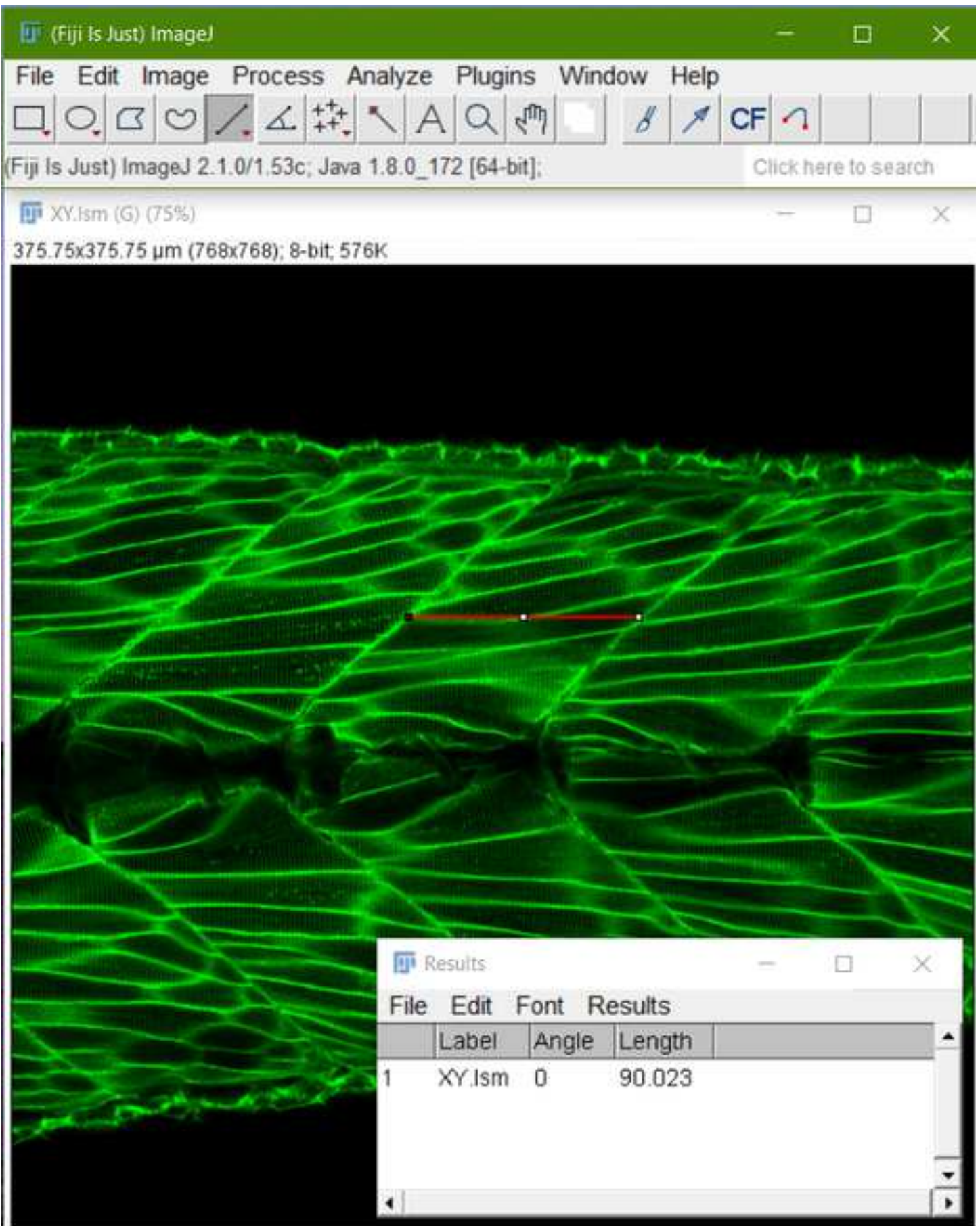


## Fish with yaw and roll









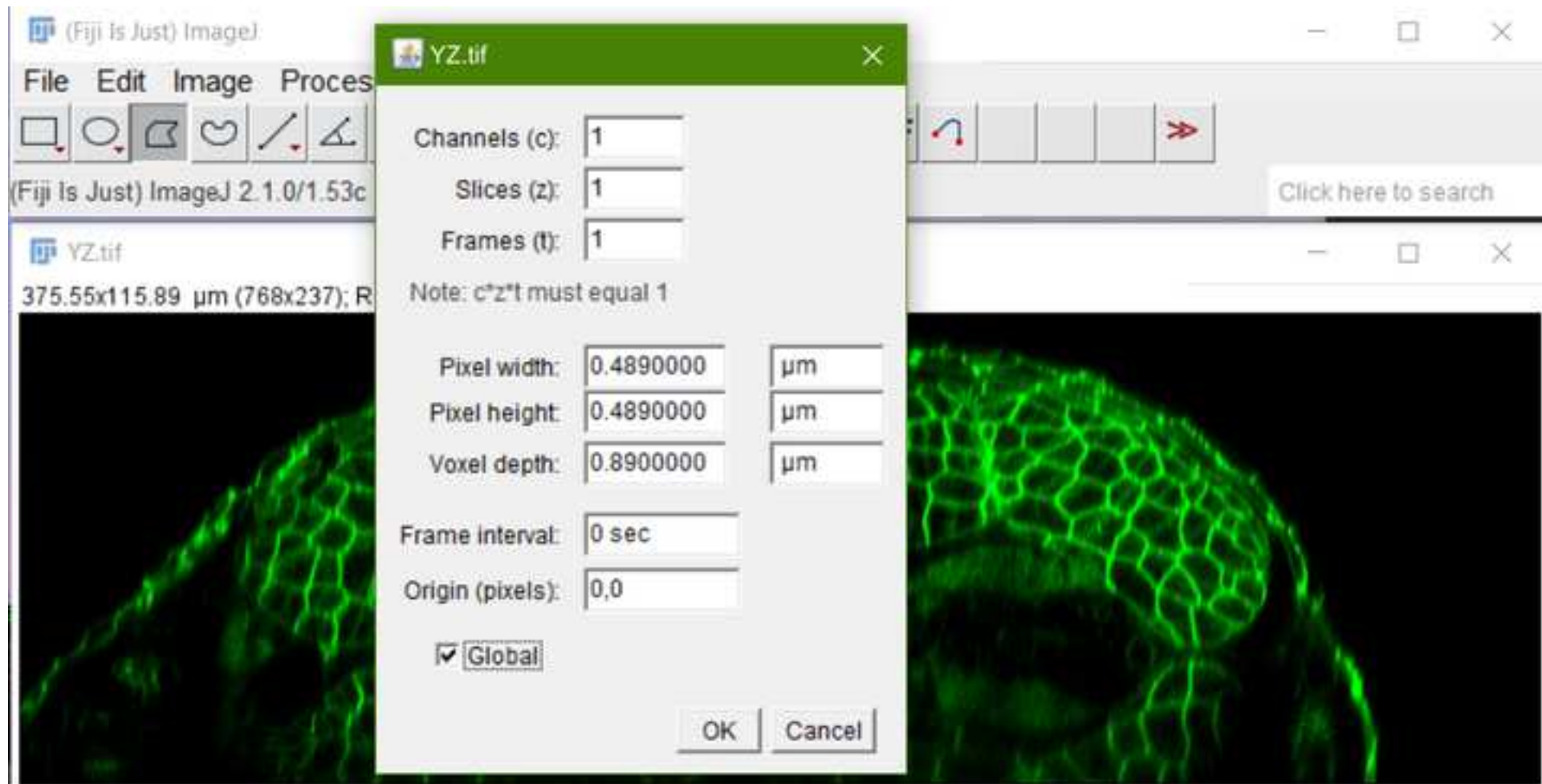
The screenshot displays the ZEN 2.3 SP1 software interface. The main window is titled "ZEN 2.3 SP1" and features a menu bar with "File", "View", "Acquisition", "Maintain", "Macro", "Tools", "Window", and "Help". A "Workspace Zoom" slider and a "Reset" button are located in the top right. Below the menu bar, there are icons for "XY.lsm" and "YZ.lsm", and a "Workspace Configuration" section with a "Reset" button.

The central panel shows the configuration for the "YZ.lsm" scan. The "Info" tab is selected, displaying the following parameters:

Name	YZ
Description	
Acquisition Date	6/15/2021 09:53:17
Notes	
User	LSM User
Scaling X	0.489 $\mu\text{m}$
Scaling Y	
Scaling Z	0.890 $\mu\text{m}$
Dimensions	x: 768, z: 130, 8-bit
Image Size	x: 375.35 $\mu\text{m}$ , z: 115.70 $\mu\text{m}$
Scan Mode	z-stack
Zoom	0.8
Objective	W Plan-Apochromat 20x/1.0 DIC (UV) VIS-IR
Position (x,y,z)	Position 1: x: 0.0 $\mu\text{m}$ , y: 0.0 $\mu\text{m}$ , z: 5.4 $\mu\text{m}$
Pixel dwell	2.13 $\mu\text{s}$
Average	line 2
Master gain	600
Digital gain	1.00
Digital offset	-0.16
Pinhole	65 $\mu\text{m}$

On the right side, the "Images and Documents" panel shows two image thumbnails. The top thumbnail is labeled "XY.lsm" with a size of 0.56 MB. The bottom thumbnail is labeled "YZ.lsm" with a size of 98 kB. Both thumbnails show green fluorescence images.

At the bottom of the interface, a status bar displays system information: "CPU 2% Free HD 0.11 TB" and "Free Ra 1.4 GB".



(Fiji Is Just) ImageJ

File Edit Image Process Analyze Plugins Window Help

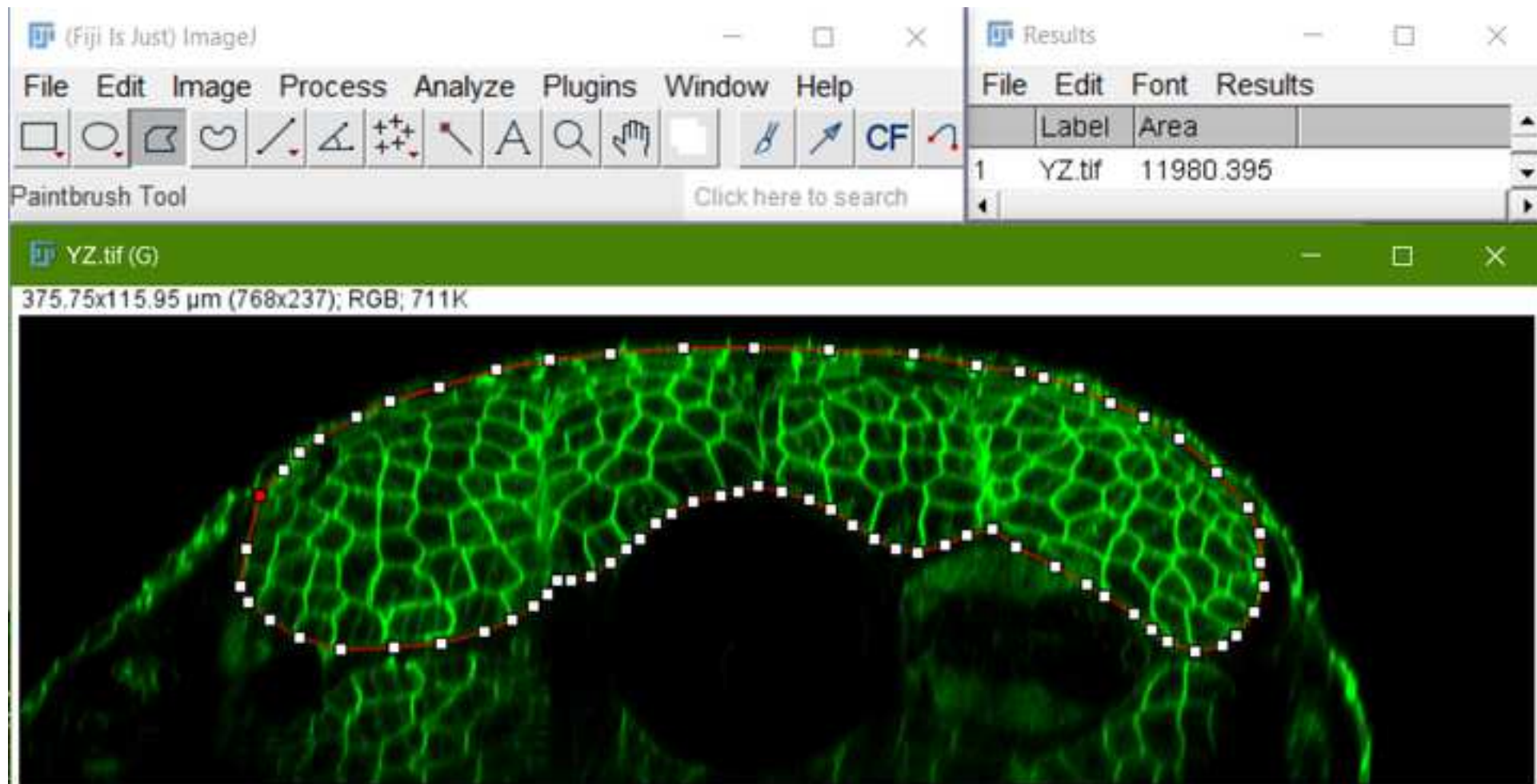
Paintbrush Tool Click here to search

Results

	Label	Area
1	YZ.tif	11980.395

YZ.tif (G)

375.75x115.95  $\mu\text{m}$  (768x237); RGB; 711K



The screenshot displays the Fiji ImageJ interface. The main window shows a green fluorescence image of a biological structure, likely a cell or tissue, with a red outline and white markers. The Results window is open, showing a table with one row: 1, YZ.tif, 11980.395. The status bar indicates the image dimensions are 375.75x115.95  $\mu\text{m}$  (768x237) and the file size is 711K.



## ARTICLE LICENSE AGREEMENT

Title of Article:

Author(s):

Title of Article:	
Author(s):	

Item 1: The Author elects to have the Article be made available (as described at <https://www.jove.com/authors/publication>) via:



Standard Access



Open Access

Item 2: Please select one of the following items:



The Author is **NOT** a United States government employee.



The Author is a United States government employee and the Article was prepared in the course of his or her duties as a United States government employee.

## ARTICLE LICENSE AGREEMENT

1. **Defined Terms.** As used in this Article License Agreement, the following terms shall have the following meanings: **"Agreement"** means this Article License Agreement; **"Article"** means the manuscript submitted by Author(s) and specified on the last page of this Agreement, including texts, figures, tables and abstracts; **"Author"** means the author who is a signatory to this Agreement; **"Collective Work"** means a work, such as a periodical issue, anthology or encyclopedia, in which the Article, along with a number of other contributions, constituting separate and independent works in themselves, are assembled into a collective whole; **"CRC License"** means the Creative Commons Attribution 4.0 Agreement (also known as CC-BY), the terms and conditions of which can be found at: <https://creativecommons.org/licenses/by/4.0/>; **"CRC NonCommercial License"** means the Creative Commons Attribution-NonCommercial 3.0 Agreement (also known as CC-BY-NC), the terms and conditions of which can be found at: <http://creativecommons.org/licenses/by-nc/3.0/legalcode>; **"Derivative Work"** means a work based upon the Article and other pre-existing works, such as a translation, musical arrangement, dramatization, fictionalization, motion picture version, sound recording, art reproduction, abridgment, condensation, or any other form in which the Article may be recast, transformed, or adapted; **"Institution"** means the institution, listed on the last page of this Agreement, by which the Author was employed at the time of the creation of the Article; **"JoVE"** means MyJove Corporation, a Delaware corporation and the publisher of Journal of Visualized Experiments; **"Parties"** means the Author and JoVE.

2. **Background.** The Author, who is the author of the Article, in order to ensure the review, Internet formatting, publication, dissemination and protection of the Article, desires to have JoVE publish the Article. In furtherance of such goals, the Parties desire to memorialize in this Agreement the respective rights of each Party in and to the Article.

3. **Grant of Rights in Article.** In consideration of JoVE agreeing to review, arrange and coordinate the peer review, format, publish and disseminate the Article, the Author hereby grants to JoVE, subject to **Sections 4 and 8** below, the exclusive, royalty-free, perpetual license (a) to publish, reproduce, distribute, display and store the Article in all forms, formats and media whether now known or hereafter developed (including without limitation in print, digital and electronic form) throughout the world, (b) to translate the Article into other languages, create adaptations, summaries or extracts of the Article or other Derivative Works or Collective Works based on all or any portion of the Article and exercise all of the rights set forth in (a) above in such translations, adaptations, summaries, extracts, Derivative Works or Collective Works and (c) to license others to do any or all of the above. The foregoing rights may be exercised in all media and formats, whether now known or hereafter devised, and include the right to make such modifications as are technically necessary to exercise the rights in other media and formats.

4. **Retention of Rights in Article.** The Author shall, with respect to the Article, retain the non-exclusive right to use all or part of the Article for the non-commercial purpose of giving lectures, presentations or teaching classes, and to post a copy of the Article on the Institution's website or the Author's personal website, in

each case provided that a link to the Article on the JoVE website is provided and notice of JoVE's copyright in the Article is included. All non-copyright intellectual property rights in and to the Article, such as patent rights, shall remain with the Author.

**5. Grant of Rights in Article – Standard Access.** This **Section 5** applies if the "Standard Access" box has been checked in **Item 1** above or if no box has been checked in **Item 1** above. In consideration of JoVE agreeing to review, arrange and coordinate the peer review, format, publish and disseminate the Article, the Author hereby acknowledges and agrees that, Subject to **Section 8** below, JoVE is and shall be the sole and exclusive owner of all rights of any nature, including, without limitation, all copyrights, in and to the Article. To the extent that, by law, the Author is deemed, now or at any time in the future, to have any rights of any nature in or to the Article, the Author hereby disclaims all such rights and transfers all such rights to JoVE.

If the Author's funding is a subject to the requirement of the NIH Public Access Policy, JoVE acknowledges that the Author retains the right to provide a copy of their final peer-reviewed manuscript to the NIH for archiving in PubMed Central 12 months after publication by JoVE. If the Author's funding is subject to the requirement of the RCUK Policy, JoVE acknowledges that the Author retains the right to self-deposit a copy of their final Accepted Manuscript in any repository, without restriction on non-commercial reuse, with a 6-month embargo, and under the CRC NonCommercial License.

Notwithstanding anything else in this agreement, if the Author's funding is a subject to the requirements of Plan S, JoVE acknowledges that the Author retains the right to provide a copy of the Author's accepted manuscript for archiving in a Plan S approved repository under a Plan S approved license.

**6. Grant of Rights in Article – Open Access.** This Section 6 applies only if the "Open Access" box has been checked in Item 1 above. If the Author's funding is subject to the requirement of the RCUK Policy, JoVE and the Author hereby grant to the public all such rights in the Article as provided in, but subject to all limitations and requirements set forth in the CRC License.

**7. Government Employees.** If the Author is a United States government employee and the Article was prepared in the course of his or her duties as a United States government employee, as indicated in **Item 2** above, and any of the licenses or grants granted by the Author hereunder exceed the scope of the 17 U.S.C. 403, then the rights granted hereunder shall be limited to the maximum rights permitted under such statute. In such case, all provisions contained herein that are not in conflict with such statute shall remain in full force and effect, and all provisions contained herein that do so conflict shall be deemed to be amended so as to provide to JoVE the maximum rights permissible within such statute.

**8. Protection of the Work.** The Author(s) authorize JoVE to take steps in the Author(s) name and on their

behalf if JoVE believes some third party could be infringing or might infringe the copyright of the Article.

**9. Privacy, Personality.** The Author hereby grants JoVE the right to use the Author's name, picture, photograph, image, biography, likeness, voice and performance in any way, commercial or otherwise, in connection with the Articles and the sale, promotion and distribution thereof.

**10. Author Warranties.** The Author represents and warrants that the Article is original, that it has not been published, that the copyright interest is owned by the Author (or, if more than one author is listed at the beginning of this Agreement, by such authors collectively) and has not been assigned, licensed, or otherwise transferred to any other party. The Author represents and warrants that the author(s) listed at the top of this Agreement are the only authors of the Article. If more than one author is listed at the top of this Agreement and if any such author has not entered into a separate Article License Agreement with JoVE relating to the Article, the Author represents and warrants that the Author has been authorized by each of the other such authors to execute this Agreement on his or her behalf and to bind him or her with respect to the terms of this Agreement as if each of them had been a party hereto as an Author. The Author warrants that the use, reproduction, distribution, public or private performance or display, and/or modification of all or any portion of the Article does not and will not violate, infringe and/or misappropriate the patent, trademark, intellectual property or other rights of any third party. The Author represents and warrants that it has and will continue to comply with all government, institutional and other regulations, including, without limitation all institutional, laboratory, hospital, ethical, human and animal treatment, privacy, and all other rules, regulations, laws, procedures or guidelines, applicable to the Article, and that all research involving human and animal subjects has been approved by the Author's relevant institutional review board.

**11. JoVE Discretion.** If more than one author is listed at the beginning of this Agreement, JoVE may, in its sole discretion, elect not to take any action with respect to the Article until such time as it has received complete, executed Article License Agreements from each such author. JoVE reserves the right, in its absolute and sole discretion and without giving any reason therefore, to accept or decline any work submitted to JoVE. JoVE has sole discretion as to the method of reviewing, formatting and publishing the Article, including, without limitation, to all decisions regarding timing of publication, if any.

**12. Indemnification.** The Author agrees to indemnify JoVE and/or its successors and assigns from and against any and all claims, costs, and expenses, including attorney's fees, arising out of any breach of any warranty or other representations contained herein. The Author further agrees to indemnify and hold harmless JoVE from and against any and all claims, costs, and expenses, including attorney's fees, resulting from the breach by the

## ARTICLE LICENSE AGREEMENT

Author of any representation or warranty contained herein or from allegations or instances of violation of intellectual property rights, damage to the Author's or the Author's institution's facilities, fraud, libel, defamation, research, equipment, experiments, property damage, personal injury, violations of institutional, laboratory, hospital, ethical, human and animal treatment, privacy or other rules, regulations, laws, procedures or guidelines, liabilities and other losses or damages related in any way to the submission of work to JoVE, or publication in JoVE or elsewhere by JoVE. All indemnifications provided herein shall include JoVE's attorney's fees and costs related to said losses or damages. Such indemnification and holding harmless shall include such losses or damages incurred by, or in connection with, acts or omissions of JoVE, its employees, agents or independent contractors.


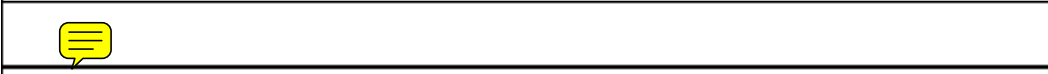

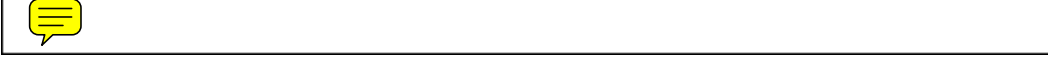


13. **Fees.** To cover the cost incurred for its work, JoVE must receive payment before publication of the

Article. Payment is due 21 days after invoice. Should the Articles not be published due to the JoVE's decision, these funds will be returned to the Author. If payment is not received before the publication of the Article, the publication will be suspended until payment is received.

14. **Transfer, Governing Law.** This Agreement may be assigned by JoVE and shall inure to the benefits of any of JoVE's successors and assignees. This Agreement shall be governed and construed by the internal laws of the Commonwealth of Massachusetts without giving effect to any conflict of law provision thereunder. This Agreement may be executed in counterparts, each of which shall be deemed an original, but all of which together shall be deemed to me one and the same agreement. A signed copy of this Agreement delivered by facsimile, e-mail or other means of electronic transmission shall be deemed to have the same legal effect as delivery of an original signed copy of this Agreement.

A signed copy of this document must be sent with all new submissions. Only one Agreement is required per submission.

### CORRESPONDING AUTHOR

Name:		
Department:		
Institution:		
Title:		
Signature:		Date: 

Please submit a **signed** and **dated** copy of this license by one of the following three methods:

1. Upload an electronic version on the JoVE submission site
2. Fax the document to +1.866.381.2236
3. Mail the document to JoVE / Attn: JoVE Editorial / 1 Alewife Center #200 / Cambridge, MA 02140